PANE

PANE Journal of Physics Education P. J. Phys. Edu. Vol 1(2), October 2026

WHAT EXACTLY IS RADIATION?

Dipankar Kaundilya*

Department of Physics, Indian Institute of Science, Bangalore-560012, Karnataka, India

*Corresponding Author: dipankark@iisc.ac.in

Abstract: This work provides a foundational review of how physics divides the universe into localized matter and propagating radiation. We unify classical electrodynamics, quantum mechanics, and general relativity under a singular mathematical language: the spatial and tensor symmetries of wavefronts. We trace how the geometry of a source dictates the outward topology of a field—moving from point-source spherical expansions governed by Laplace's spherical harmonics to line-source cylinders, conical shockwaves, and infinite plane waves. We introduce Heitler's gauge separation alongside the Power-Zienau-Woolley (PZW) unitary transformation to establish the exact boundaries of radiative multipole expansions, extending the framework to nuclear gamma channels, relativistic continuous acceleration engines, and statistical blackbody cavity fields. Finally, we explore the mechanical boundaries where pure geometry fails and quantum mechanics takes over, analyzing radiation pressure, Doppler cooling limits, macroscopic phase-locking in Dicke Superradiance, and the complete suppression of motional radiation within the quantum Lamb-Dicke regime.

Keywords: electrodynamics; Gauge separation; massless field excitations; Lamb-Dicke regime

(Received: 15 September 2026; accepted: 29 October 2026; published: 30 October 2026)

1 Introduction

The physical universe is fundamentally partitioned into two distinct dynamic expressions: localized matter and propagating radiation. We define "matter" as localized energy densities that act as static or quasi-static sources, whereas "radiation" is defined strictly as the completely decoupled, asymptotic transport of energy fleeing toward infinity. Within the scope of this pedagogical survey, this classification serves as a operational working framework optimized for electromagnetic and gravitational field configurations, rather than an exhaustive partition of all physical matter states.

To preserve the absolute mathematical rigor of this field-theoretic boundary, we explicitly exclude particulate nuclear ejections, such as α and β radiation, from this framework. Because α and β emissions are massive, charged leptons and hadrons possessing substantial localized rest mass, their macroscopic propagation properties are governed by de Broglie matter waves with highly localized momentum footprints. Consequently, this paper restricts its taxonomy strictly to pure gauge field and tensor configurations: the propagation of massless electromagnetic waves and spacetime perturbations whose outward geometries are direct reflections of their generative engines.

The spatial and geometric footprint of radiation is not arbitrary; rather, it acts as a direct mathematical mirror of the source's internal geometric changes over time. By tracking these geometric transformations across classical electrodynamics, quantum mechanics, and general relativity, we can map the trajectory of propagating energy from basic classical point sources up to extreme limits of quantum atomic confinement and cosmic-scale thermodynamic relics.

2 Distinction between Matter and Fields

The concept of wave-particle duality for the observable universe has certain ontological problems, because any localized packet of momentum can exhibit wave-like behavior and any propagating wave envelope can be resolved into discrete energy quanta as defined by the de Broglie relation $p = \frac{h}{\lambda}$. Therefore, this duality presents a persistent ambiguity in the description of reality.

To establish an unambiguous classification suitable for physics research, the constituents of the universe must be categorized by their underlying quantum statistical nature, algebraic representations and spin-parity states. This approach separates the universe into two distinct classes: Matter (Spinor Fields) and Radiation (Gauge and Tensor Fields).

2.1 Spinor Fields

Matter is composed of half-integer intrinsic angular momentum entities called Spin $(s = \frac{1}{2}, \frac{3}{2}...)$ These entities are described by Spinor fields (Ψ) and they obey Fermi-Dirac statistics $n_i = \frac{1}{e^{\frac{(\epsilon_i - \mu)}{k_B T}} + 1}$ and are structurally governed by the Pauli-Exclusion Principle.

For an assembly of identical fermions the total wave function must be completely anti-symmetric under the permutation of any two particle coordinates $x_i \equiv (r_i, \sigma_i)$ where r_i represents position and σ_i tracks the spin projection. If two identical fermions attempt to occupy the exact same quantum state $(x_i = x_j)$ the mathematical relation dictates $\Psi = -\Psi$ forcing the probability density to vanish identically. $\Psi(x_1, ...x_i, ...x_j, ...x_n) = -\Psi(x_1, ...x_j, ...x_i, ...x_n)$ or $\hat{P_{ij}}\Psi = -\Psi$. This restriction generates a non-local purely quantum mechanical exchange interaction that prohibits two identical fermions from occupying the same complete single-particle state, including the spin projection, though it does not preclude overlapping spatial distributions[1].

Fields are classified by how they transform under a spatial rotation through an angle θ around an axis $\hat{n}$ governed by the rotation operator $R(\theta) = e^{-\frac{i\theta\hat{n}.J}{\hbar}}$. A scalar field $(\text{spin}-0)$ remains unchanged under rotation. A vector field (spin-1) such as the electric field E, transforms like a spatial arrow, rotating the vector by 2π returns the vector exactly to its initial state. $R(2\pi)V = +V$. Conversely, a spinor field (Ψ) acts mathematically as the square root of a vector. When a spinor field undergoes a full 2π rotation it picks up a global negative sign $R(2\pi)\Psi = -\Psi$. To return a spinor field exactly back to its initial phase state, the system must undergo a 4π rotation $R(4\pi)\Psi = +\Psi$. This phase reversal property under 2π rotation is the geometric origin of fermionic anti-symmetry. Swapping the positions of two identical fermions is topologically equivalent to a 2π rotation of their relative coordinates, forcing the wavefunction sign inversion. This topological phase difference between standard and non-orientable manifolds is visually mapped as a pedagogical analogy in Figure 1[2].

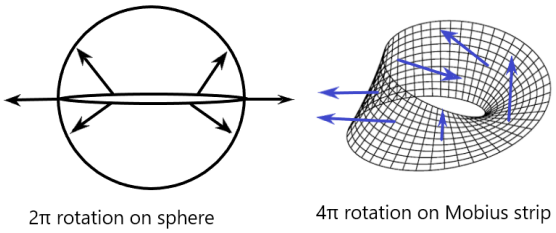


Figure 1: Pedagogical analogy of spatial rotation symmetries in orientable vs. non-orientable manifolds. (Left) A standard vector field mapped on a sphere returns to its original identity configuration after a trivial 2π spatial rotation. (Right) A normal vector field tracked along a Möbius strip encounters a topological phase inversion after a 2π circuit, requiring a double-cover 4π loop to achieve a full identity return.

While scalar and vector fields are governed by the Klein-Gordon and Maxwell equations respectively, the fundamental spinor field of electron is governed by the Dirac equation:

$$(i\hbar\gamma^\mu\partial_\mu - mc)\Psi = 0 \tag{1}$$

Here Ψ is a 4-component Dirac spinor. These four complex components do not represent coordinates in $(3+1)$ dimensional physical spacetime (ct, x, y, z). Instead, they represent the intrinsic structural degrees of freedom of the field. (Electron spin up↑, down↓, Positron spin up↑, down↓). Because fermions cannot occupy the same complete single-particle quantum state, they are forced to stack hierarchically into distinct energy levels (atomic orbitals, nuclear shells, degenerate fermi seas and gases). This structural stacking underpins the fixed volume of the periodic elements, the stability of chemical bonds and the macroscopic boundary layers of solid matter. Thus, spinor fields function as the localized anchors of mass and charge density in the universe.

2.2 Bosonic Fields

Bosons are composed of integer intrinsic angular momentum entities called Spins$(s = 0, 1, 2..)$ They are described by gauge or tensor fields and obey Bose-Einstein statistics $n_i = \frac{1}{e^{\frac{(\epsilon_i - \mu)}{k_B T}} - 1}$ and are completely exempted from the Pauli Exclusion principle.

The multibody state vector for an assembly of identical bosons remains completely symmetric under coordinate permutations. $\hat{P_{ij}}\Psi = +\Psi$ or $\Psi(x_1, ...x_i, ...x_j, ...x_n) = +\Psi(x_1, ...x_j, ...x_i, ...x_n)$ This symmetry allows an infinite number of bosonic excitations to occupy the exact same spatial mode and quantum state simultaneously. $R(2\pi)A = +A$. This capability enables microscopic quantum field fluctuations to build up coherently into macroscopic classical fields, observed as electromagnetic waves and gravitational waves. Pedagogically, this transition to a classical-field description occurs when a massive occupation of bosons builds into a coherent state—a quantum superposition of displacement operator excitations where the field operators approximate their classical macroscopic expectation values with minimal phase uncertainty [3].

True radiation corresponds to the dynamical excitations of these bosonic fields that completely decouple from their fermionic spinor sources and propagate independently towards infinity. Radiation does not maintain a static, localized position in space, instead, it redistributes energy, momentum and angular momentum across the spacetime manifold at or near the cosmic speed limit c. Note that spin–statistics classification applies to both fundamental and composite particles. In this article, we restrict our definition of radiation to outgoing excitations of massless gauge and tensor fields.

For a bosonic field to qualify as true radiation rather than a localized short range interaction (such as the weak $W^{\pm}$ and Z^0 gauge bosons), it must exhibit masslessness $(m = 0)$. Under Special Relativity, masslessness restricts a particle's spin vector to align parallel or anti-parallel to its momentum vector, reducing the spin projection to two discrete helicity states $(h = \pm s)$. This constraint governs the physical radiation channels.

Spin $- 0$ (Hypothetical Massless Scalar Radiation) Characterized by a single helicity state $(h = 0)$. While the physical Standard Model Higgs boson is massive [4] and its associated Goldstone modes are swallowed to provide longitudinal polarization for the weak gauge bosons [5, 6], a hypothetical massless scalar field serves as a fundamental model for evaluating monopole radiation fields. It propagates isotropically and lacks directional polarization vectors.

Spin $- 1$ (Vector Gauge Radiation-Photons) They mediate classical electromagnetic radiation (A_μ). Because $(m = 0)$, the longitudinal polarization state is suppressed, leaving only two transverse helicity states $(h = \pm 1)$. These manifest macroscopically as left and right handed circular polarization.

Spin-2 (Tensor Radiation-Gravitons) They mediate gravitational waves $(h_{\mu\nu})$. Masslessness isolates two physical transverse polarization modes $(h = \pm 2)$, macroscopically observed as the plus (+) and cross (x) strains of the spacetime metric.

To summarize our operational field-theoretic taxonomy within this defined scope, the algebraic particle statistics (fermion vs. boson) and the physical manifestations of radiation are synthesized structurally in Table 1.

3 Radiation Generation Mechanisms

We know two different mechanisms for generation of electromagnetic waves. One mechanism occurs when an electron makes a transition from an upper energy level to a lower energy level, emitting photons with an energy equal to the energy gap. The other occurs when a charged particle undergoes acceleration or deceleration, emitting a continuous stream of photons, as seen in an X-ray (Bremsstrahlung). Now at a glance these two mechanisms look so different but at the fundamental level we can find some common denominator between them. Essentially, these localized fermionic spinor fields are shaking off bosonic gauge fields either via classical acceleration or quantum transition so we must integrate them into a single field theoretic framework. We may theorize that the escaping bosonic field does not care whether its source is a changing quantum wavefunction or a classical current density. In fact both systems shake off radiation by driving time-dependent charges in the underlying current density a process governed by the coupling of spinor sources to the vector gauge field.

Table 1: Algebraic and Structural Classification of Matter and Fields

Statistical Class	**Structural Type**	**Examples**	**Physical Role in Paper**
Spinor Fields	Fundamental Lepton	$e^-, \mu, \tau, \nu_e, \nu_\mu, \nu_\tau$	Localized Mass/Charge Anchors
(Fermions, $s = \frac{1}{2}$)	Fundamental Quark	u, d, c, s, t, b	Strong-force Field Sources
	Composite Baryon	Proton, Neutron, Hyperons	Nuclear Core / Matter Boundaries
Bosonic Fields	Composite Meson	$J/\psi, \pi, K$	Localized Energy Packets
(Bosons, $s = 0, 1, 2$)	Massless Gauge Field	Photons (A_μ)	Vector Electromagnetic Radiation
	Massless Tensor Field	Gravitons ($h_{\mu\nu}$)	spacetime Tensor Radiation

3.1 Field of a moving charge

Attach a reference frame S' with a charge moving at constant velocity v along the x-axis with respect to the lab frame S. We assume that the origins of two inertial frames coincide at $t = 0$. Mark an observation point (x', y') where we would like to see the field due to point charge. Note that in this frame charge q is at rest and hence it would not generate any magnetic field. The geometric orientation of both inertial frames and the observation point is illustrated in Figure 2.

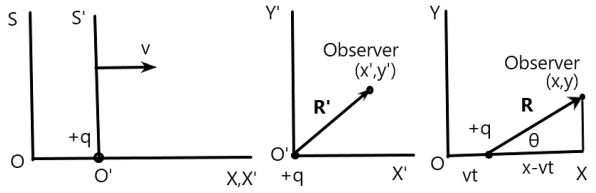


Figure 2: Geometrical framing of a point charge in uniform linear motion. The reference frame S' is anchored directly to the charge $+q$ moving at constant velocity v, while frame S acts as the stationary laboratory frame mapping the field components toward an observation point (x, y).

So electric field

$$\vec{E'} = \frac{1}{4\pi\epsilon_0}\frac{q}{(R')^2}\hat{R'} = \frac{kq}{(R')^3}\vec{R'} \tag{2}$$

where we have set $k = \frac{1}{4\pi\epsilon_0}$

We use field transformation equations to find out the relation between fields in two ordinary SI inertial frames:

$$Ex = E'_x \quad \text{and} \quad Ey = \gamma\left(E'_y - vB'_z\right) \quad \text{where} \quad \gamma = \frac{1}{\sqrt{1-(v/c)^2}} \tag{3}$$

So we get

$$Ex = E'_x = \frac{kqx'}{(R')^3} \quad \text{and} \quad Ey = \gamma E'_y = \frac{k\gamma q y'}{(R')^3} \quad \text{as } B'_z = 0 \tag{4}$$

As $\vec{R'} = x'\hat{i} + y'\hat{j}$

So

$$(R')^2 = x'^2 + y'^2 = \gamma^2(x - vt)^2 + y^2 \tag{5}$$

Using Lorentz transform $x' = \gamma(x - vt)$ and $y' = y$

Then

$$E_x = \frac{kqx'}{(R')^3} = \frac{kq\gamma(x - vt)}{[\gamma^2(x - vt)^2 + y^2]^{3/2}} \tag{6}$$

$$E_y = \frac{kq\gamma y}{[\gamma^2(x - vt)^2 + y^2]^{3/2}} \tag{7}$$

As

$$\vec{E} = E_x\hat{i} + E_y\hat{j} = (kq\gamma)\frac{(x - vt)\hat{i} + y\hat{j}}{[\gamma^2(x - vt)^2 + y^2]^{3/2}} \tag{8}$$

We know $\vec{R} = (x - vt)\hat{i} + y\hat{j}$ and $R^2 = (x - vt)^2 + y^2$

Also

$$y = R\sin\theta \quad \text{hence} \quad (x - vt)^2 = R^2(1 - \sin^2\theta) \tag{9}$$

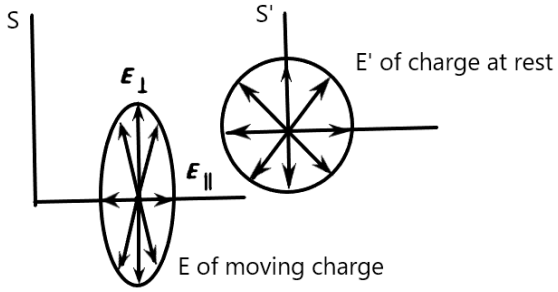


Figure 3: Vector distribution profile of the electric field lines emanating from a moving charge. The schematic demonstrates the geometric deformation of the field profile, comparing the parallel electric field $E_{\parallel}$ along the axis of linear motion to the compressed perpendicular field components $E_{\perp}$.

And then we can simplify

$$\frac{kq\gamma\vec{R}}{[\gamma^2R^2(1 - \sin^2\theta) + R^2\sin^2\theta]^{3/2}} = \frac{kq\gamma\vec{R}}{R^3\gamma^3(1 - \frac{v^2}{c^2}\sin^2\theta)^{3/2}} \tag{10}$$

Hence we get

$$\vec{E} = \frac{kq\vec{R}}{R^3}\frac{(1 - \frac{v^2}{c^2})}{(1 - \frac{v^2}{c^2}\sin^2\theta)^{3/2}} \quad \text{as} \quad 1 - \frac{v^2}{c^2} = \frac{1}{\gamma^2} \tag{11}$$

Therefore for $\theta = 0, \pi$,

$$E_{\parallel} = \frac{kq}{R^2}\left(1 - \frac{v^2}{c^2}\right) = \frac{kq}{R^2}\frac{1}{\gamma^2} \quad \text{and} \tag{12}$$

and for $\theta = \frac{\pi}{2}$,

$$E_{\perp} = \frac{kq}{R^2}\frac{1}{\sqrt{1 - \frac{v^2}{c^2}}} = \frac{kq}{R^2}\gamma \tag{13}$$

The resulting compression of these electric field lines perpendicular to the motion is shown in Figure 3.

Now we discuss the emission of radiation from an accelerating charge. We set up a charge q to be at rest at $t = 0$. It is then accelerated with a constant acceleration a for small duration Δt and then continues to move with the constant velocity achieved thereafter. The electric field lines for the charge at rest emanate radially outward we denote its field by E_0 and the lines from charge moving at constant velocity are also somewhat radial and are denoted by E_v. Note that E_0 and E_v electric fields are time-independent. It is the transient field E_{rad} which is time-dependent and gives rise to the radiation and propagates with speed c. This has spherical shape and it behaves as plane waves for large distances. The formation of this transient kink in the field lines is depicted in Figure 4.

So we determine the radiation field E_{rad} at an instant t and position r. Assume that $t \gg \Delta t$ and $v \ll c$. Therefore, the displacement by source (charge) vt is very small compared to distance traveled by the radiation wavefront, $vt \ll ct$. It is due to this reason we consider the field lines for moving charge E_v and the stationary charge E_0 to be parallel to each other. Next, we find the congruent triangles formed by the radiation field and acceleration. We establish $\frac{E_\perp}{E_\parallel} = \frac{v_\perp t}{c\Delta t}$, where $E_\perp, E_\parallel$ are components of E_{rad}, $c\Delta t$ is the distance traveled by radiation wave during the small time interval for which the charge was accelerated, and $v_\perp t$ is the displacement of the charge over time t in the direction perpendicular to the wave propagation. Hence $v_\perp = a_\perp \Delta t$ and $t = \frac{r}{c}$.

And we obtain

$$\frac{E_\perp}{E_\parallel} = \frac{(a_\perp \Delta t)(\frac{r}{c})}{c\Delta t} = \frac{a_\perp r}{c^2} \tag{14}$$

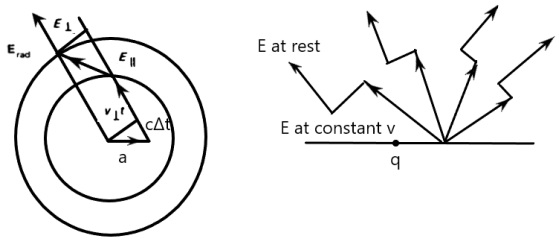


Figure 4: Geometric footprint of the radiation field generated by a briefly accelerated charge. The diagram maps the propagation of the transient transverse wave component E_{rad} spreading outward at speed c, bridging the stationary radial lines E_0 and the shifted fields E_v of the moving charge within the accelerated boundary layer $c\Delta t$.

By using Gaussian pillbox parallel to $E_\parallel$ and noting that the box is free from charges for this consideration we immediately get

$$E_\parallel = E_v = \frac{kq}{r^2} \quad \text{and thereby} \quad E_\perp = \frac{kq}{c^2}\frac{a_\perp}{r} \tag{15}$$

Since $E_\parallel$ is time-independent, it is not included in the radiation wave. Thus radiation field is a transverse wave. Finally we write

$$E_{\text{rad}}(r,t) = -\frac{kq}{c^2}\frac{a_\perp(t')}{r} \tag{16}$$

where $t' = t - \frac{r}{c}$ is an instant earlier than t when the charge underwent acceleration and $-$ve sign indicates the opposite direction of E_{rad} and a.

3.2 Asymptotic Field Isolation and the Larmor Radiation Threshold

Because electromagnetic field propagates at finite speed of c, the fields observed at a distant point $\vec{r}$ at time t depends on the position, velocity and acceleration of the charge at an earlier retarded time t_r. This causal boundary condition is defined implicitly by the constraint equation $t_r = t - \frac{|r - r'(t_r)|}{c}$. When a point charge q moves with a relativistic velocity $\beta(t_r) = \frac{v(t_r)}{c}$, it compresses or dilates its own field signal along the observation vector $\hat{n}$. This kinematic compression alters the simultaneously observed source volume by an apparent factor, yielding the exact Lienard-Wiechart scalar potential Φ and vector potential A. The exact causal vector configuration between the past retarded position and the present observer is traced in Figure 5.

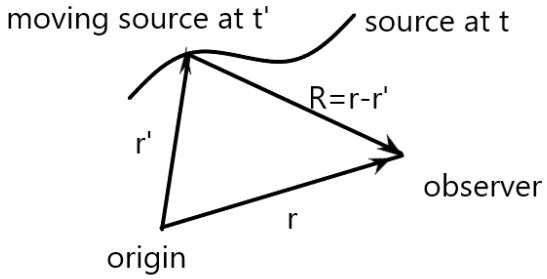


Figure 5: Geometrical configuration of the Liénard-Wiechert potentials. The electromagnetic field observed at position r and time t is determined entirely by the retarded position r' and kinematic state of the source charge at the earlier retarded time t'.

$$\Phi(r,t) = \frac{1}{4\pi\epsilon_0}\left[\frac{q}{(1-\hat{n}.\vec{\beta})|r-r'|}\right]_{t_r} \tag{17}$$

$$\vec{A}(r,t) = \frac{\mu_0}{4\pi}\left[\frac{qv}{(1-\hat{n}.\vec{\beta})|r-r'|}\right]_{t_r} \tag{18}$$

The math of Liénard-Wiechert potentials also behaves in a similar manner because it relies on a nested, self-referential time loop:

$$c(t-t_r) = |\mathbf{r}-\mathbf{r}'(t_r)| = R(t_r) \tag{19}$$

Differentiate both sides with respect to the observer time t:

$$c\left(1-\frac{dt_r}{dt}\right) = \frac{dR}{dt_r}\frac{dt_r}{dt} \tag{20}$$

We have $R^2 = (\mathbf{r}-\mathbf{r}')\cdot(\mathbf{r}-\mathbf{r}')$. Hence:

$$2R\frac{dR}{dt_r} = 2(\mathbf{r}-\mathbf{r}')\cdot\left(-\frac{d\mathbf{r}'}{dt_r}\right) = -2\mathbf{R}\cdot\mathbf{v}(t_r) \tag{21}$$

$$\frac{dR}{dt_r} = -\hat{\mathbf{n}}\cdot\mathbf{v}(t_r) \tag{22}$$

Now on back-substitution:

$$c\left(1-\frac{dt_r}{dt}\right) = -(\hat{\mathbf{n}}\cdot\mathbf{v})\frac{dt_r}{dt} \tag{23}$$

Thus we get

$$\frac{dt_r}{dt} = \frac{1}{1-\hat{n}\cdot\vec{\beta}} \tag{24}$$

The factor $(1-\hat{n}\cdot\vec{\beta})$ acts as a dynamic scaling factor. It compresses the electric field lines in front of a moving charge and stretches them behind it. Even though the particle's actual charge never changes, its effective charge density fluctuates dynamically because the math is forced to map a past history onto a present observation moment.

Differentiating these potentials with respect to space and time yields the electric field $E(r,t) = -\nabla\Phi(r,t) - \frac{\partial A(r,t)}{\partial t}$. We also need to apply the chain rule to account for the implicit retarded time dependency $(t_r = t - R/c)$. On doing this, the total field splits into two distinct components

$$\mathbf{E}_{\text{near}} = \frac{q}{4\pi\epsilon_0}\left[\frac{\mathbf{n}-\boldsymbol{\beta}}{\gamma^2(1-\boldsymbol{\beta}\cdot\mathbf{n})^3R^2}\right]_{\text{ret}} \tag{25}$$

$$\mathbf{E}_{\text{far}} = \frac{q}{4\pi\epsilon_0 c}\left[\frac{\mathbf{n}\times\left[(\mathbf{n}-\boldsymbol{\beta})\times\dot{\boldsymbol{\beta}}\right]}{(1-\boldsymbol{\beta}\cdot\mathbf{n})^3R}\right]_{\text{ret}} \tag{26}$$

where $R = |r - r'(t_r)|$ and $\gamma = (1-\beta^2)^{-1/2}$

In continuous systems, such as an electron decelerating through the Coulomb field of an atomic nucleus, i.e. braking radiation or (Bremsstrahlung) the acceleration vector $a(t)$ changes smoothly. This smooth modification shakes free a continuous unbroken spectrum of bosonic field excitations. To scale this framework from discrete point kinematics to macroscopic continuous systems, we explicitly isolate the escaping radiation field from the static self-fields bound to the moving source, we evaluate the total electric field $\mathbf{E}(\mathbf{r},t)$ derived from the Liénard-Wiechert potentials [7]. By performing the explicit differentiation with respect to the retarded time t_r, the total field splits uniquely into two structurally distinct geometric components:

$$\mathbf{E}(\mathbf{r},t) = \mathbf{E}_{\text{near}}(\mathbf{r},t) + \mathbf{E}_{\text{far}}(\mathbf{r},t) \tag{27}$$

The first component, the velocity or near-field, depends strictly on the instantaneous velocity $\boldsymbol{\beta} = \mathbf{v}/c$ of the charge distribution (25). Because $\mathbf{E}_{\text{near}}$ exhibits an inverse-square spatial dependency ($\mathbf{E}_{\text{near}} \propto 1/R^2$), its contribution to the asymptotic Poynting flux $\oint \mathbf{S}\cdot d\mathbf{A}$ scales as $1/R^4 \times R^2 d\Omega \propto 1/R^2$. As a consequence, $\lim_{R\to\infty}\oint \mathbf{S}_{\text{near}}\cdot d\mathbf{A} = 0$, proving that the velocity field represents non-radiative, localized energy densities that remain rigidly anchored to the matter source [7].

Conversely, true propagating radiation is governed entirely by the acceleration or far-field component, which scales linearly with the time derivative of the velocity $\dot{\boldsymbol{\beta}}$ (26).

Because the acceleration field falls off slowly as a first-order spatial inverse ($\mathbf{E}_{\text{far}} \propto 1/R$), the associated radiation Poynting vector $\mathbf{S}_{\text{far}} = \frac{1}{\mu_0}(\mathbf{E}_{\text{far}} \times \mathbf{B}_{\text{far}})$ drops off as $1/R^2$. When integrated over a boundary sphere of radius R, the surface area element $dA = R^2 d\Omega$ perfectly cancels this geometric attenuation:

$$P(u) = \lim_{R\to\infty}\oint \mathbf{S}_{\text{far}}\cdot\mathbf{n}\,R^2 d\Omega = \text{constant} \tag{28}$$

This constant flux confirms that $\mathbf{E}_{\text{far}}$ completely decouples from the source coordinate system to carry energy asymptotically to infinity [7]. Crucially, this limit compares the outgoing signal at a fixed retarded time $u = t - R/c$. While the integrated flux evaluates to a constant value across a given wavefront shell, the total power $P(u)$ may still vary dynamically over the duration of a pulse profile, rather than representing an entirely time-independent emission. In the non-relativistic limit ($\beta \ll 1, \gamma \to 1$), this acceleration field simplifies to the classical transverse profile:

$$\mathbf{E}_{\text{far}} \approx \frac{q}{4\pi\epsilon_0 c^2 R}\left[\mathbf{n}\times(\mathbf{n}\times\dot{\mathbf{v}})\right] = \frac{qa\sin\theta}{4\pi\epsilon_0 c^2 R}\hat{\boldsymbol{\theta}} \tag{29}$$

Integrating the resulting Poynting vector over all solid angles yields the classical Larmor power distribution formula:

$$P = \frac{q^2 a^2}{6\pi\epsilon_0 c^3} \tag{30}$$

This formula holds strictly for a non-relativistic point charge accelerating in a vacuum, confirming that the generation of free, non-local bosonic excitations requires a broken state of inertial motion ($\mathbf{a} \neq 0$). The Larmor formulation serves as an operational threshold in our taxonomy: it marks the boundary line where localized electromagnetic self-fields transform into a fully decoupled, independent macroscopic radiation field gas [7].

3.3 Quantum Transition Dynamics and Selection Rules

In the atomic regime, an electron does not travel along a classical spatial trajectory $r'(t)$, meaning it lacks a traditional acceleration vector $a(t)$. Instead, it transitions between stationary eigenstates of a localized fermionic system. Despite this conceptual shift, the underlying mathematical framework that drives radiation remains identical: a time-dependent oscillation in the system's current density.

Consider a spinor field transitioning from an initial state $|\psi_i(r,t)\rangle = |\psi(r)\rangle\, e^{-\frac{iE_i t}{\hbar}}$ to final state $|\psi_f(r,t)\rangle = |\psi_f(r)\rangle\, e^{-\frac{iE_f t}{\hbar}}$. During the quantum jump, the system exists in a time-dependent coherent superposition $|\psi_{\text{total}}(r,t)\rangle = c_i\,|\psi_i(r,t)\rangle + c_f\,|\psi_f(r,t)\rangle$. Evaluating the quantum mechanical charge probability density $\rho = q|\,|\psi_{\text{total}}\rangle\,|^2$ reveals an explicit time-dependent oscillation occuring at the Bohr transition frequency $\omega_0 = \frac{E_i - E_f}{\hbar}$

$$\rho(r,t) = q\left[|c_i|^2|\,|\psi_i\rangle\,|^2 + |c_f|^2|\,|\psi_f\rangle\,|^2 + 2\text{Re}(c_i^* c_f\,|\psi_i\rangle^*\,|\psi_f\rangle\, e^{-i\omega_0 t})\right] \tag{31}$$

This interference term generates a real oscillating transition charge density and a matching transition current density $J_{fi}(r,t)$ given as:

$$J_{fi}(r,t) = \frac{q\hbar}{2im}\left[|\psi_f\rangle^*\,\nabla\,|\psi_i\rangle - (\nabla\,|\psi_f\rangle^*)\,|\psi_i\rangle\right] e^{-i\omega_0 t} \tag{32}$$

This equation proves that during a quantum transition the atom acts as a virtual microscopic AC antenna. The transition current density oscillates at frequency ω_0 serving at the source term that drives Maxwell's wave equations. Examples of these transition configurations mapping to atomic dipoles and quadrupoles are shown in Figure 6.

By treating the radiation field as a quantized gauge perturbation governed by the interaction Hamiltonian $H_{\text{int}} = -\int \mathbf{J}\cdot\mathbf{A}\, d^3r$, the transition rate W_{if} is derived via Fermi's Golden Rule $W_{if} = \frac{2\pi}{\hbar}|\langle f|H_{\text{int}}|i\rangle|^2\rho(E_f)$.

In the long wavelength limit (the electric dipole approximation) this expression reduces to the transition dipole matrix element $\mathbf{p}_{fi} = \langle f|q\mathbf{r}|i\rangle$. The average power radiated during this quantum transition matches the semi-classical Larmor result $P = \frac{\mu_0\omega_0^4}{3\pi c}|\mathbf{p}_{fi}|^2$.

It is important to emphasize that spontaneous emission from an initially excited energy eigenstate does not involve a classical macroscopically oscillating mean dipole $\langle\hat{\mathbf{p}}\rangle = 0$; rather, the radiation is driven entirely by the underlying quantum transition current density matrix element $\mathbf{J}_{fi}$.

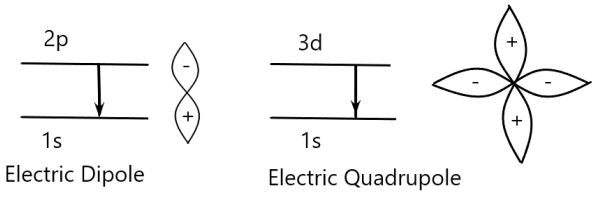


Figure 6: Representation of atomic state transitions as microscopic multipole radiation sources. (Left) The 2p to 1s transition establishes an oscillating asymmetric charge profile acting as an electric dipole. (Right) The 3d to 1s transition establishes a four-lobed spatial inversion profile acting as an electric quadrupole.

In the quantum mechanical regime, the transition of a spinor field between an initial state $|i\rangle$ and a final state $|f\rangle$ emits or absorbs a single bosonic gauge excitation. The probability of this transition is governed by the matrix element $\langle f|\hat{H}_{\text{int}}|i\rangle$.

The spatial parity operator $\hat{P}$ reflects all spatial coordinates through the origin ($\mathbf{r} \to -\mathbf{r}$). Spherical harmonics exhibit a definite parity under this transformation, scaling as:

$$\hat{P}Y_{\ell m}(\theta,\phi) = (-1)^\ell Y_{\ell m}(\theta,\phi) \tag{33}$$

Consider a symmetric system consisting of two identical accelerated charges or an atom with an initial and a final state that share identical parity ($\hat{P}|i\rangle = \pm|i\rangle$ and $\hat{P}|f\rangle = \pm|f\rangle$). The electric dipole operator $\hat{\mathbf{p}} = q\hat{\mathbf{r}}$ has odd spatial parity ($\hat{P}\hat{\mathbf{r}} = -\hat{\mathbf{r}}$). Evaluating the transition matrix element yields:

$$\langle f|\hat{\mathbf{r}}|i\rangle = \int \psi_f^*(\mathbf{r})\ \mathbf{r}\psi_i(\mathbf{r})d^3r \tag{34}$$

Because the total integrand is the product of an even function ($\psi_f^*\psi_i$) and an odd function ($\mathbf{r}$), it integrates to zero over all space, completely suppressing the electric dipole channel ($\ell = 1$). To satisfy energy conservation during an isolated, undriven single-photon decay, the emitted quantum carries an energy strictly dictated by the atomic gap: $\hbar\omega_\gamma = E_i - E_f = \hbar\omega_0$, forcing the system to bypass the $E1$ limit via higher-order single-photon channels (such as $M1$ or $E2$) without changing the fundamental emission frequency ω_0 [8, 9, 10]. However, the frequency-doubled signature ($2\omega_0$) can be physically realized within the atomic regime if the framework is extended to multi-quantum dynamics. Specifically, if the atomic system is continuously driven by an external laser field at a foundational frequency ω_0, the simultaneous absorption of two photons can induce a non-linear transition across same-parity states. The resulting non-linear localized transition current density oscillates at exactly twice the foundational driving frequency ($2\omega_0$), shaking off a frequency-doubled secondary field. Alternatively, in an un-driven configuration, the system can undergo a spontaneous two-photon decay where two entangled photons are emitted simultaneously to satisfy $\hbar\omega_1 + \hbar\omega_2 = \hbar\omega_0$, satisfying the strict selection rules $|J_i - J_f| \leq L \leq J_i + J_f$.

This angular coupling and mode filtering is formalized exactly by the **Wigner-Eckart theorem**. The theorem factorizes the complete transition matrix element of any arbitrary multipole tensor operator $\hat{T}_q^k$ into a structural component and a pure spatial geometric component:

$$\langle j_f m_f|\hat{T}_q^k|j_i m_i\rangle = \frac{\langle j_f||\hat{T}^k||j_i\rangle}{\sqrt{2j_f+1}}\langle j_i m_i\, kq|j_f m_f\rangle \tag{35}$$

Here, the reduced matrix element $\langle j_f||\hat{T}^k||j_i\rangle$ isolates the internal radial wavefunctions bound to the specific dynamics of the spinor source. Conversely, the **Clebsch-Gordan coefficients** $\langle j_i m_i\, kq|j_f m_f\rangle$ serve as the algebraic backbone of selection rules, mapping the angular momentum coupling between the initial state $|j_i m_i\rangle$, the final state $|j_f m_f\rangle$ and the emitted bosonic gauge quantum $|kq\rangle$.

The Wigner-Eckart framework demonstrates that selection rules are not merely abstract constraints on particle hopping, but rigid spatial boundary conditions. The Clebsch-Gordan coefficient mathematically handles the pure spacetime geometry of the interaction, locking the allowed emission channels exclusively to matching physical topologies of the emerging radiation wavefront.

3.4 Spherical Harmonics as the Geometric Unifier

The mathematical unification of classical acceleration fields and discrete quantum jumps is completed by mapping their angular and topological expressions onto spherical Harmonics $Y_{lm}(\theta, \phi)$. These specialized functions are the native, non-divergent solutions to the angular component of the Laplacian operator on a 2-D sphere $\Lambda^2 Y_{lm} = -l(l+1)Y_{lm}$. Because these boundary modes are dictated by spatial geometry rather than energy quantization they serve as the foundational mathematical building blocks for expanding escaping fields. Crucially, a clear distinction must be maintained between these scalar basis functions and the actual directional intensity profiles of vector electromagnetic radiation. Wavefronts represent surfaces of constant phase, whereas physical radiation intensity is governed by the outward, time-averaged Poynting flux $\langle \mathbf{S} \rangle = \frac{1}{\mu_0}\langle \mathbf{E} \times \mathbf{B} \rangle$. For instance, while the squared magnitude of the scalar harmonic $|Y_{10}|^2 \propto \cos^2\theta$ peaks along the polar axis, a physical vector electric dipole aligned along the z-axis radiates an intensity profile proportional to $\sin^2\theta/R^2$, [11, 12] vanishing completely along its axis of motion.

Isotropic, boundaryless localized systems naturally emit concentric spherical wavefronts. Connecting individual scalar harmonics to physical vector fields requires appropriate angular derivatives and vector combinations—such as vector spherical harmonics—to correctly account for polarization and directional energy flux. The mathematical basis profiles of these scalar functions are tracked for reference in Figure 7, mapping how the structural index

degree (l) representing total radiated angular momentum and order (m) tracking spatial projection define the geometric lobes of the basis topologies. To mathematically construct this, we begin with the homogeneous Helmholtz wave equation for a scalar field component $\psi(\mathbf{r})$:

$$\left(\nabla^2 + k^2\right)\psi(\mathbf{r}) = 0 \tag{36}$$

By employing the Green's function decomposition and expanding via the spherical Bessel-Addition Theorem, the radial and angular components cleanly decouple.

$$R'' + \frac{2}{r}R' + \left[k^2 - \frac{l(l+1)}{r^2}\right]R = 0 \tag{37}$$

$$\left[\frac{1}{\sin\theta}\frac{d}{d\theta}\left(\sin\theta\frac{d}{d\theta}\right) + \frac{1}{\sin^2\theta}\frac{d^2}{d\phi^2} + l(l+1)\right]Y_l^m(\theta,\phi) = 0 \tag{38}$$

General solution

$$\psi(r,\theta,\phi) = \sum_{l=0}^{\infty}\sum_{m=-l}^{+l}(a_{lm}j_l(kr) + b_{lm}y_l(kr))Y_l^m(\theta,\phi) \tag{39}$$

The spatial angular dependence of the radiation is completely mapped by the scalar spherical harmonics $Y_{lm}(\theta,\phi)$. Here, the structural index degree (l) represents the total radiated angular momentum, while the order (m) denotes its spatial projection along the quantization axis.

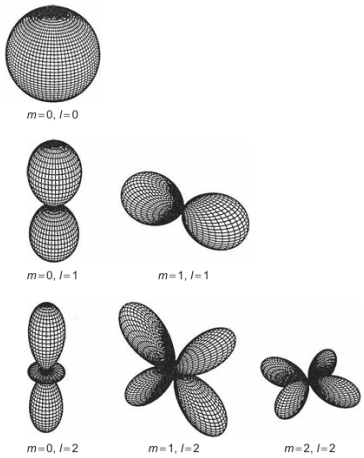


Figure 7: Mathematical basis profiles and angular tracking patterns of orthogonal scalar spherical harmonics. The degree (ℓ) dictating total radiated angular momentum and order (m) tracking spatial projection define the geometric lobes of the basis functions, rather than representing direct vector field radiation intensity profiles.

Spherical Symmetries and the Architecture of Multipole Radiation To connect this localized acceleration field $\mathbf{E}_{\text{far}}$ to our structural expansion modes, we evaluate a compact source distribution ($d \ll \lambda$) within the non-relativistic limit ($\beta \ll 1$). Expanding the retarded time dependency $t_r = t - |\mathbf{r} - \mathbf{r}'|/c$ allows the far-field acceleration term to be decomposed into an infinite series of time-dependent source moments. The lowest-order term isolates the system's net dipole acceleration $\ddot{\mathbf{p}}$, while subsequent spatial corrections isolate higher-order tensor structures like the quadrupole engine $\dddot{\mathbf{Q}}$. When these vector fields are cast onto an isotropic, boundaryless geometry, they naturally project their specific angular tracking parameters onto the orthogonal basis functions of the wave equation.

In classical electrodynamics, the far-field vector potential $\mathbf{A}(\mathbf{r}, t)$ generated by a localized, time-varying current density $\mathbf{J}(\mathbf{r}', t')$ is evaluated by expanding the retarded time constraint. For a source oscillating at an angular frequency ω with an associated wavenumber $k = \omega/c$, the far-field potential at an observation position $\mathbf{r}$ is expressed as:

$$\mathbf{A}(\mathbf{r}, t) = \frac{\mu_0}{4\pi} \frac{e^{i(kr-\omega t)}}{r} \int \mathbf{J}(\mathbf{r}') e^{-ik\hat{\mathbf{n}}\cdot\mathbf{r}'} d^3r' \tag{40}$$

where $\hat{\mathbf{n}}$ is a unit vector pointing toward the observer.

When the physical dimensions of the source are much smaller than the wavelength of the emitted radiation ($kr' \ll 1$), the exponential retardation phase factor can be expanded as a Taylor series:

$$e^{-ik\hat{\mathbf{n}}\cdot\mathbf{r}'} = \sum_{n=0}^{\infty} \frac{(-ik)^n}{n!} (\hat{\mathbf{n}} \cdot \mathbf{r}')^n = 1 - ik(\hat{\mathbf{n}} \cdot \mathbf{r}') - \frac{k^2}{2}(\hat{\mathbf{n}} \cdot \mathbf{r}')^2 + \dots \tag{41}$$

This spatial power series maps directly onto the spherical harmonic index ℓ. The $n = 0$ term isolates the $\ell = 1$ Electric Dipole channel, projecting an angular footprint proportional to $Y_{1m}(\theta, \phi)$. The $n = 1$ term isolates the quadratic spatial variations ($\mathbf{r}'^2$), generating a four-lobed cloverleaf pattern mapped by the $Y_{2m}(\theta, \phi)$ harmonics.

As the source velocity approaches the speed of light ($\beta \to 1$), this long-wavelength approximation fails. The retarded time factor $(1 - \hat{\mathbf{n}} \cdot \boldsymbol{\beta})^{-3}$ acts as a geometric mixer. Instead of isolating a single clean multipole, the relativistic engine mixes an infinite ladder of spherical harmonics ($\sum C_\ell Y_{\ell m}$) simultaneously, distorting the symmetric dipole donut into a highly asymmetric, forward-beamed searchlight cone.

3.5 The Unified Current Operator

Superficially, radiation generation appears split into two fundamentally distinct physical paradigms: the discrete, quantum-mechanical transition of an electronic spinor between localized bound states ($\Delta E = \hbar\omega$), and the continuous, classical acceleration of a macroscopic charge distribution (e.g., Bremsstrahlung or synchrotron engines) [7]. At the fundamental field-theoretic level, however, these mechanisms share an identical mathematical denominator. The escaping bosonic gauge field is indifferent to whether its driver is a shifting quantum wavefunction or a classical trajectories manifold; both systems radiate by establishing a time-dependent current density vector $j^\mu(x)$ that couples directly to the gauge potential $A_\mu(x)$ [7].

This common denominator is formalized by the gauge-invariant interaction action:

$$S_{\text{int}} = -\frac{1}{c} \int j^\mu(x) A_\mu(x)\, d^4x \tag{42}$$

where $j^\mu = (c\rho, \mathbf{j})$ acts as the source term for the gauge field. The divergence of this field establishes charge conservation ($\partial_\mu j^\mu = 0$). The transition between regimes depends entirely on the formulation of this current density operator:

The Classical Continuum Limit: For a point source moving along a deterministic worldline $x_0^\mu(\tau)$, the current density behaves as a localized distribution constrained by Dirac delta functions:

$$j^\mu_{\text{class}}(x) = qc \int_{-\infty}^{\infty} \frac{dx_0^\mu(\tau)}{d\tau} \delta^4\left(x - x_0(\tau)\right) d\tau \tag{43}$$

When integrated into the retarded Green's functions of the wave equation, this time-dependent vector current generates the continuous spectral fields of classical electrodynamics, governed by the Liénard-Wiechert potentials and Larmor's acceleration power distribution.

The Quantum Transition Limit: For an elementary spinor field undergoing a transition between an initial state Ψ_i and a final state Ψ_f, the classical current is replaced by the transition current matrix element of Quantum Electrodynamics (QED):

$$j^\mu_{fi}(x) = cq\bar{\Psi}_f(x)\gamma^\mu\Psi_i(x) \tag{44}$$

where γ^μ denotes the Dirac matrices. This transition matrix element oscillates dynamically at the Bohr frequency $\omega_{fi} = \omega_0 = (E_i - E_f)/\hbar$.

Consequently, a quantum transition is not an instantaneous, non-local jump; rather, it is a period of quantum superposition where the interference between state envelopes creates a localized, time-dependent charge-current oscillation. Pedagogically, while this transition current couples to the vacuum modes of the transverse vector field via Fermi's Golden Rule to shake off discrete gauge excitations (photons), a clear distinction must be maintained when describing this as a microscopic antenna; spontaneous emission from an initially excited energy eigenstate does not involve a classical, macroscopically oscillating mean dipole ($\langle \hat{\mathbf{p}} \rangle = 0$), but is driven purely by the matrix elements of the transition current density operator $j^{\mu}_{fi}(x)$. The resulting angular distribution of the emitted fields remains dictated entirely by the underlying spatial symmetry of this transition current matrix element.

4 Gauge Invariance

Because the coupling of both classical and quantum currents to the vector field potential A_μ forms the absolute structural bedrock of our radiation architecture, we must ensure that our mathematical formulations remain invariant under arbitrary field transformations. This structural baseline is governed entirely by the principles of gauge freedom. To trace how this filtering mechanism systematically isolates real physical radiation from unphysical parts of spacetime vectors, we begin by reviewing Maxwell's equations, examining them both in the presence of localized sources and within a pure, sourceless vacuum:

In the presence of sources ($\rho \neq 0, J \neq 0$)

$$\nabla \cdot E = \frac{\rho}{\epsilon_0} \tag{45}$$

$$\nabla \cdot B = 0 \tag{46}$$

$$\nabla \times E = -\frac{\partial B}{\partial t} \tag{47}$$

$$\nabla \times B = \mu_0 J + \frac{1}{c^2}\frac{\partial E}{\partial t} \tag{48}$$

In Vacuum ($\rho = 0, J = 0$)

$$\nabla \cdot E = 0 \tag{49}$$

$$\nabla \cdot B = 0 \tag{50}$$

$$\nabla \times E = -\frac{\partial B}{\partial t} \tag{51}$$

$$\nabla \times B = \frac{1}{c^2}\frac{\partial E}{\partial t} \tag{52}$$

By taking the curl of the vacuum relation and applying the vector identity $\nabla \times (\nabla \times \vec{E}) = \nabla(\nabla \cdot \vec{E}) - \nabla^2 \vec{E}$, we can exploit the sourceless condition ($\nabla \cdot \vec{E} = 0$) to uncouple the fields into independent homogeneous wave equations:

$$\nabla^2 \vec{E} = \frac{1}{c^2}\frac{\partial^2 \vec{E}}{\partial t^2} \quad \text{and} \quad \nabla^2 \vec{B} = \frac{1}{c^2}\frac{\partial^2 \vec{B}}{\partial t^2} \tag{53}$$

The directional transport of the energy density $u = \frac{1}{2}\left(\epsilon_0 E^2 + \frac{1}{\mu_0}B^2\right)$ carried forward by these decoupling wavefronts is governed by Poynting's conservation theorem $\left(\frac{\partial u}{\partial t} + \nabla \cdot \vec{S} = 0\right)$, where the escaping energy and linear momentum flux are driven strictly by the transverse cross-product:

$$\vec{S} = \frac{1}{\mu_0}(\vec{E} \times \vec{B}) \quad \text{and} \quad \vec{p}_{\text{field}} = \frac{\vec{S}}{c^2} \tag{54}$$

In nature, the real physical entities are the electric field (E) and the magnetic field (B). They act upon a charge via Lorentz force

$$F = qE + qv \times B \tag{55}$$

However to simplify the description of Maxwell's equations we invent two different potentials, scalar (Φ) and vector (A) defined as

$$B = \nabla \times A \quad \text{and} \quad E = -\nabla\Phi - \frac{\partial A}{\partial t} \tag{56}$$

Now, notice a mathematical loophole because the curl of any gradient is zero

$$\nabla \times (\nabla\chi) = 0 \tag{57}$$

we can change A and Φ by adding any arbitrary mathematical function $\chi(r,t)$ to them as

$$A \to A + \nabla\chi \quad \text{and} \quad \Phi \to \Phi - \frac{\partial\chi}{\partial t} \tag{58}$$

If we plug these altered potentials back into the formulas for E and B, the function χ completely cancels out. Thus, the real field does not change at all.

Therefore, we define a gauge as the specific choice that one makes for the arbitrary function χ. Because the physical universe does not care what χ is, the theory possesses Gauge Invariance. There are infinitely many ways to describe the exact same physical reality.

But why do we need them in the first place? We could have simply worked with E and B fields, why do we need potentials after all? It is because potentials contain more information than fields. In simple terms, field is force per unit charge, whereas potential is energy per unit charge and energy contains more information about the system than the forces, that is why we have developed Lagrangian and Hamiltonian formalisms. For instance, the Schrodinger equation does not know how to interact with E and B fields directly. Therefore, we write the Hamiltonian of a charged mass point (q,m) interacting with an electromagnetic field using potentials via the minimal coupling scheme

$$H = \frac{1}{2m}(p - qA)^2 + q\Phi \tag{59}$$

If we send a charged particle across a field free region (in the vicinity of a completely shielded solenoid) where $(E = 0, B = 0)$ but $(A \neq 0)$ the particle's wavefunction detects the presence of the source, that is it feels the vector potential even when the fields are zero.

So for quantum mechanics we do need potentials and the moment we use them we inherit the gauge freedom. We also know that relativity demands $(3{+}1)$ dimensions for Lorentz Covariance so we have potentials as a four-vector $(A^\mu = (\frac{\Phi}{c}, A)$. We also know that a photon is a massless spin-1 vector boson. A traveling photon can only have two polarization states (up and down and left and right to the direction of motion), so how do we eliminate those 2 extra components prescribed by relativity. We do that by picking a suitable gauge either Coulomb or Lorentz. We create a constraint that removes one unphysical degree of freedom. And by using the charge conservation we remove the other unphysical degree of freedom. Thus, it is in this sense that we need gauge theory to filter out the unphysical parts of spacetime vectors such that only real physical radiation remains.

Let's see the idea of gauge freedom by solving two different choices of gauges. Firstly let's take $\chi(r,t) = e^{-t^2}\sin(r^2)$ where $r^2 = x^2 + y^2 + z^2$. So we have to prove that $\nabla \times (\nabla\chi) = 0$. We evaluate

$$\nabla\chi = \frac{\partial\chi}{\partial r}\hat{r} = [2re^{-t^2}\cos(r^2)]\hat{r} \tag{60}$$

Then we find out the curl in spherical polar coordinate

$$\nabla \times F(r,\theta,\phi) = \frac{1}{r\sin\theta}\left[\frac{\partial}{\partial\theta}(F_\phi\sin\theta) - \frac{\partial F_\theta}{\partial\phi}\right]\hat{r} + \frac{1}{r}\left[\frac{1}{\sin\theta}\frac{\partial F_r}{\partial\phi} - \frac{\partial}{\partial r}(rF_\phi)\right]\hat{\theta} + \frac{1}{r}\left[\frac{\partial}{\partial r}(rF_\theta) - \frac{\partial F_r}{\partial\theta}\right]\hat{\phi} \tag{61}$$

Now $\nabla\chi = F_r\hat{r}$ so we do not have any F_θ, F_ϕ terms so $\frac{\partial F_r}{\partial\phi} = 0$, $\frac{\partial F_r}{\partial\theta} = 0$ hence the curl reduces to

$$\nabla \times (\nabla\chi) = \frac{1}{r\sin\theta}\left[\frac{\partial}{\partial\theta}(0) - \frac{\partial}{\partial\phi}(0)\right]\hat{r} + \frac{1}{r}\left[\frac{1}{\sin\theta}\frac{\partial}{\partial\phi}(F_r) - 0\right]\hat{\theta} + \frac{1}{r}\left[0 - \frac{\partial}{\partial\theta}(F_r)\right]\hat{\phi} = 0 \tag{62}$$

Hence $B = B_0$. Now we have to show that $\nabla \frac{\partial \chi}{\partial t} = \frac{\partial}{\partial t}(\nabla \chi)$

So we first perform $\frac{\partial \chi}{\partial t} = -2te^{-t^2}\sin(r^2)$ then

$$\nabla\left(\frac{\partial \chi}{\partial t}\right) = \frac{\partial}{\partial r}(-2te^{-t^2}\sin(r^2))\hat{r} = [-4tre^{-t^2}\cos(r^2)]\hat{r} \tag{63}$$

We already have $\nabla\chi = [2re^{-t^2}\cos(r^2)]\hat{r}$; so

$$\frac{\partial}{\partial t}(\nabla\chi) = [-4tre^{-t^2}\cos(r^2)]\hat{r} \tag{64}$$

Hence we get

$$E = E_0 + \left[\nabla\left(\frac{\partial \chi}{\partial t}\right) - \frac{\partial}{\partial t}(\nabla\chi)\right] = E_0 + 0 = E_0 \tag{65}$$

What does this show? It shows that even if a gauge function is spherically symmetric to a radiating system (like a breathing charged shell) it still manages to carry zero physical field with it. Let's take another example $\chi(r,t) = \frac{e^{-t^2}}{r^2}$ note that we have a singularity at $r = 0$. So for $r > 0$,

$$\nabla\chi = \frac{\partial}{\partial r}\left(\frac{e^{-t^2}}{r^2}\right) = -\frac{2e^{-t^2}}{r^3}\hat{r} \tag{66}$$

Again because this gradient field is purely along the radius vector it has no angular dependence hence its curl is identically zero $\nabla \times (\nabla\chi) = 0$. Also

$$\nabla\left(\frac{\partial \chi}{\partial t}\right) = \frac{\partial}{\partial t}(\nabla\chi) = \frac{4te^{-t^2}}{r^3}\hat{r} \tag{67}$$

Subtracting these two paths yields zero ensuring $E = E_0$ and $B = B_0$.

What does this gauge function reveal? It tells that for a gauge transformation to be globally valid, the scalar function χ must be continuously differentiable across the entire domain. Because $\chi = \frac{e^{-t^2}}{r^2}$ blows up to infinity at $r = 0$, it is not a valid global gauge transformation. If in some problem charge is staying at origin we cannot apply such a gauge otherwise the vector potential $A = A_0 + \nabla\chi$ develops an unwanted singularity that acts like an imaginary magnetic dipole kept at the origin. To see what it does to the scalar potential, observe that

$$\Phi = \Phi_0 - \frac{\partial \chi}{\partial t} = \Phi_0 + \frac{2te^{-t^2}}{r^2} \tag{68}$$

Notice that as $r \to 0$, the scalar potential spikes to infinity, meaning the potential looks non-local even if the real fields are localized.

Now we come to the choice of Coulomb and Lorentz gauge for the description of electrodynamics or other kind of fields. So we naturally ask which gauge is better? Actually neither gauge is more realistic than the other because gauges are completely unphysical constructs. Nature does not care which gauge we select, if we build an antenna or an ion trap the measured values for the real fields E and B and the energy flowing into the detector will be identical down to the last significant figures in both the constructs. However depending on what aspect of physics we want to probe the choice of gauge does have a say.

Coulomb Gauge: ($\nabla \cdot \mathbf{A} = 0$) (Spatial divergence of vector potential is zero) This choice reduces the Maxwell equation to

$$\nabla^2\Phi = -\frac{\rho}{\epsilon_0}, \quad \text{and} \quad \Box\mathbf{A} = -\mu_0\mathbf{J}_T \tag{69}$$

Under this gauge we have only two polarizations of a photon because it eliminates the longitudinal and scalar modes. The remaining vector potential contains only two transverse polarizations observed in real-world experiments. While it separates the electrostatic potential Φ attached to the charge from the transverse vector potential $\mathbf{A}$, it is critical to note that $\mathbf{A}$ matches a purely independent, homogeneous escaping radiation wave only in the sourceless asymptotic limit; inside the source domain ($\mathbf{J}_T \neq 0$), transversality alone does not imply pure radiation, as the transverse field still retains localized near-zone induction contributions. This gauge we will utilize later for our discussions on Heitler's decomposition and PZW transformation [13].

Paradox: We get an illusion of non-locality under this gauge, because Poisson's equation for Φ contains no time derivative, if a charge moves locally at some place, its scalar potential Φ gets updated across the edge of the universe instantaneously which seems to violate relativity. The paradox is resolved however when we calculate $E = -\nabla\Phi - \frac{\partial A}{\partial t}$, the time derivative of the vector potential A generates an equal and opposite instantaneous component that perfectly destroys the superluminal signal, ensuring that the real measurable field obeys causality.

Lorentz Gauge: $\partial_\mu A^\mu = 0$ This choice treats space and time on equal footing preserving Lorentz Covariance. By uncoupling the scalar and vector potentials it forces the Maxwell equations into

$$\Box\Phi = -\frac{\rho}{\epsilon_0} \quad \text{and} \quad \Box A = -\mu_0 J \tag{70}$$

This gauge honors causality. If a source moves, a wave of potential propagates outward with speed c. Everything is dictated by the retarded time

$$t_{\text{ret}} = t - \frac{|r - r'|}{c} \tag{71}$$

naturally generating the Lienard-Wiechert potentials. It presents a world view where information cannot travel faster than light.

Paradox: By forcing the four-vector potential $A^\mu = (\frac{\Phi}{c}, A)$ to be treated symmetrically the math introduces unphysical degrees of freedom. The field vector permits four types of polarizations of photon, two transverse, one longitudinal and one scalar (time component). The latter two are "ghost states"–unphysical polarizations that carry negative probabilities. To fix this and recover real physics, calculations must be patched up with constraints such as Ward identities in linear covariant Abelian frames, or extended to Faddeev–Popov ghosts in non-Abelian manifolds, to force non-physical states to cancel out each other [14]. But we will use this gauge for our treatment of gravity waves and QED.

4.1 Gauge Separation Thresholds

Physical reality is invariant under arbitrary gauge transformations (χ). We utilize specific gauges to isolate unphysical degrees of freedom. Now we select the radiation gauge or Coulomb gauge $(\nabla \cdot A = 0)$. We further decompose the electric field into a non-radiative longitudinal part E_L, (a static extension of the source), and a transverse part E_T which will carry the true propagating radiation.

We write the total electric field in terms of the potentials:

$$E = -\nabla\Phi - \frac{\partial A}{\partial t} \tag{72}$$

We impose the Coulomb gauge condition. This gauge requires the vector potential to be strictly divergence free (Solenoidal) $\nabla.A = 0$ We define two separate vector fields from total electric field equation, the Longitudinal component $E_L = -\nabla\Phi$. This component is purely irrotational because the curl of any gradient is identically zero $\nabla \times E_L = -\nabla \times (\nabla\Phi) = 0$. And the Transverse component $E_T = -\frac{\partial A}{\partial t}$. This component is purely solenoidal because the spatial divergence operator commutes with the time derivative: $\nabla \cdot E_T = -\nabla \cdot (\frac{\partial A}{\partial t}) = -\frac{\partial}{\partial t}(\nabla \cdot A) = 0$

So we have $E = E_L + E_T$. Let's prove that they are indeed orthogonal. That is $\int E_L \cdot E_T d^3r = 0$

$$\int_{\text{all space}} E_L \cdot E_T d^3r = \int_{\text{all space}} (-\nabla\Phi) \cdot \left(-\frac{\partial A}{\partial t}\right) d^3r = \int_{\text{all space}} \nabla\Phi \cdot \frac{\partial A}{\partial t} d^3r \tag{73}$$

We utilize vector calculus identity for the divergence of a scalar times a vector $\nabla \cdot (\Phi V) = \nabla\Phi \cdot V + \Phi(\nabla \cdot V)$

We rewrite the integrand where $V = \frac{\partial A}{\partial t}$

$$\nabla\Phi \cdot \frac{\partial A}{\partial t} = \nabla \cdot \left(\Phi \frac{\partial A}{\partial t}\right) - \Phi \left(\nabla \cdot \frac{\partial A}{\partial t}\right) \tag{74}$$

Back-substituting this result into the volume integral over all space

$$\int E_L \cdot E_T d^3r = \int \nabla \cdot \left(\Phi \frac{\partial A}{\partial t}\right) d^3r - \int \Phi \left(\frac{\partial}{\partial t}(\nabla \cdot A)\right) d^3r \tag{75}$$

Evaluate the integral layers. The second term collapses to zero. Because due to Coulomb gauge ($\nabla \cdot A = 0$), so its time derivative is also zero which entirely eliminates this term. The first term collapses via Gauss divergence theorem. We convert the remaining volume integral into a bounding surface integral at infinity.

$$\int_{\text{all space}} \nabla \cdot \left(\Phi \frac{\partial A}{\partial t}\right) d^3r = \oint_{\text{surface at}\infty} \left(\Phi \frac{\partial A}{\partial t}\right) \cdot dS \tag{76}$$

For physically localized charge distributions the potentials drop off asymptotically at infinity ($\Phi \sim 1/r$ and $A \sim 1/r$, while the surface area scales as r^2. The integrand falls off as $1/r \cdot 1/r^2 = 1/r^3$, meaning the surface integral vanishes to zero as $r \to \infty$. Thus we prove $\int_{\text{all space}} E_L \cdot E_T d^3r = 0$.

This confirms that the longitudinal and transverse field components occupy completely independent orthogonal vector subspaces in Hilbert space.

This separation reveals the structure of the electric field, we call $\mathbf{E}_L$ as the non-radiative part because it is a longitudinal extension which does not propagate toward infinity. It is governed by the Poisson's equation $\nabla^2\Phi = -\frac{\rho}{\epsilon_0}$ and evaluated as a gradient $\mathbf{E}_L = -\nabla\Phi$. Although this component lacks intrinsic, propagating wave-like time derivatives in its governing equation, it is not necessarily a strictly static matter extension; a dynamically changing charge density $\rho(\mathbf{r}, t)$ will produce a time-dependent longitudinal field that updates instantaneously across the domain, whose unphysical superluminal signal is subsequently canceled out by matching induction terms in the transverse vector potential updates $\mathbf{E}_T = -\frac{\partial \mathbf{A}}{\partial t}$ [15].

E_T is the transverse component of the total electric field. It is driven by vector potentials updates $E_T = -\frac{\partial A}{\partial t}$. It satisfies the homogeneous wave equation, therefore, it propagates energy and momentum asymptotically towards infinity.

So what benefits do we reap after such a decomposition of the electric field of a moving charge. For that to explore let's see how does a stationary charge interacts with a time varying electromagnetic field. We use the Minimal Coupling scheme to build a model of interaction. We write the Hamiltonian as $H = \frac{(p-qA)^2}{2m} + q\Phi$. We see after inspection that the Hamiltonian contains $(p \cdot A)$ kind of interaction. We know that vector potential is rich in physics. It is a vector quantity which can be associated with every point in space. It can be a function of position $A(r)$ as well as a function of velocity $A(v)$. When it works as $A(r)$ it is like a stationary vector field staying at every point. But when it works as $A(v)$ it will have time dependence and therefore we get a time varying vector field connecting electric and magnetic fields at every point in space. It is this kind of vector potentials which bring bending in the trajectory of the electric and magnetic field lines. We know such kind of bending in the circular motion where the particle is changing velocity at every point along the tangent, in such motion we cannot change the kinetic energy of the particle but its trajectory changes due to velocity's direction change. Now let's look at our minimal coupling Hamiltonian:

$$\frac{(p - qA)^2}{2m} = \frac{p^2}{2m} - \frac{q}{2m}(p \cdot A + A \cdot p) + \frac{q^2}{2m}A^2 \tag{77}$$

So we see linear interaction terms $p \cdot A$ and quadratic diamagnetic terms A^2 which will generate unphysical states. So we transform to a more feasible framework of $d \cdot E$ and $m \cdot B$ interaction when the dipole moment or any other higher multipole moments couples with the electric field or magnetic field. As these quantities can be well measured so we prefer to work in this framework.

For that to achieve we start with unitary generator $U = \exp(-\frac{i}{\hbar}\int P \cdot A d^3r)$, if we define $S = \int P \cdot A d^3r$ then our operator becomes $U = \exp(-\frac{i}{\hbar}S)$ where $P(r)$ is polarization density vector $P(r) = d\delta^3 r$ where $d = qr$. We write the new transformed Hamiltonian as

$$H_{PZW} = H_{matter} + H_{field} - \frac{1}{\varepsilon_0}\int P \cdot D\, d^3r - \int M \cdot B\, d^3r \tag{78}$$

For simplicity let's work with the electric field only then under electric dipole approximation where spatial field variations over the atomic dimensions are neglected $A(r)$ is constant, and the polarization field reduces to $P = qr\delta r$. Then the scalar generator simplifies to $S = qr \cdot A = d \cdot A$

And the PZW Hamiltonian is reduced to minimal Hamiltonian transformation $H_{\text{PZW}} = UH_{\text{min}}U^\dagger$
Then we perform BCH expansion

$$UOU^\dagger = O - \frac{i}{\hbar}[S, O] + \frac{1}{2!}\left(-\frac{i}{\hbar}\right)^2 [S, [S, O]] - \dots \tag{79}$$

We also have the commutation relations $[r, S] = 0$ hence $UrU^\dagger = r$ and $[A_i, A_j] = 0$ hence $UAU^\dagger = A$ and $[S, p] = i\hbar qA$ so $UpU^\dagger = p - \frac{i}{\hbar}(i\hbar qA) = p + qA$

$$U\left[\frac{(p - qA)^2}{2m}\right]U^\dagger = \frac{1}{2m}(UpU^\dagger - qUAU^\dagger)^2 = \frac{1}{2m}(p + qA - qA)^2 = \frac{p^2}{2m} \tag{80}$$

Hence the PZW transform isolates the pure kinetic term $\frac{p^2}{2m}$. The linear parametric coupling $(p \cdot A)$ is completely nullified. The non-local quadratic diamagnetic term A^2 is eliminated from the kinetic energy operator. We make a note at this point that however the A^2 term is not destroyed rather it is systematically absorbed into the field's self energy. Field conjugate momentum $[A, \Pi] = i\hbar\delta(r - r')$ and $U\Pi U^\dagger = \Pi + P$. Utilizing the transverse canonical field commutator $[A_i(r), \Pi_j(r')] = i\hbar\delta^T_{ij}(r - r')$ [16], the Baker–Campbell–Hausdorff expansion yields a positive shift:

$$\frac{1}{2\epsilon_0}\int(\Pi + P)^2 d^3r = \frac{1}{2\epsilon_0}\int \Pi^2 d^3r + \frac{1}{\epsilon_0}\int \Pi \cdot P d^3r + \frac{1}{2\epsilon_0}\int P^2 d^3r \tag{81}$$

The last term represents the self polarization energy of the electric field itself. This term relocates the interaction energy strictly to the localized multipole parameters $d \cdot E$, shifting the quadratic coupling into a static localized polarization self energy term P^2.

5 Radiation From Confined Particles

When N atoms are packed tightly inside a sub-wavelength volume ($V \ll \lambda^3$), individual atomic emitters lose their statistical independence, and phase-lock into entangled states. The ensemble acts collectively as a unified, macroscopic "macro-atom" linked via common vacuum modes.

Rather than emitting undecoupled light with randomized, uncorrelated phases where the total power scales linearly ($\propto N$), the system locks into collective, highly entangled states known as Dicke States [17]. This phase-locking mechanism drives cooperative spontaneous emission, forcing the maximum radiated peak power to scale quadratically: $P \propto N^2$, which represents a collective peak-power effect assuming symmetric coupling of all emitters to a single common radiation field mode within a sub-wavelength volume, while total energy conservation is strictly maintained throughout the system decay. Conversely, when the system transitions to fermionic channels, quantum statistics bound the emission to a strict linear limit [18].

The geometry of the underlying atomic cloud dictates the outward spatial symmetry of the radiated field. An isotropic spherical atomic cloud preserves a spherical emission symmetry (Y_{1m}) while heavily accelerating the overall state decay rate. Conversely, a highly anisotropic, pencil-shaped atomic cloud operates as an "end-fire" antenna array. It automatically synthesizes and directs the collective quantum burst into a highly directional, planar-like wavefront segment. On a cosmological scale, this phase-locking mechanism appears in spinning Kerr black holes, where relativistic superradiant scattering processes across the ergosphere extract rotational spacetime energy to amplify passing spin-2 gravitational wave modes; it is critical to note that while the atomic system

relies on collective multi-body state coherence, black hole superradiance acts instead as a purely kinematic wave amplification mechanism that extracts energy directly from the rotating spacetime metric without requiring phase-locked emitter states [19].

5.1 The Momentum of Fields and the Classical-to-Quantum Shift

Radiation fields carry both energy and linear momentum, defined fundamentally by the relativistic field relation ($p = \frac{E}{c}$). This field momentum is mechanically transferred to physical matter whenever light is absorbed, reflected, or scattered by a target source. The physical manifestation of this momentum transfer shifts fundamentally across operational regimes:

Classical Continuum Regime: Continuous radiation pressure exerts a smooth, macroscopic Lorentz force distributed evenly across large physical structures, such as Crookes radiometers and space-travel solar sails.

Quantum Mechanical Regime: Energy and momentum transfer completely resolves into discrete, localized momentum kicks ($\hbar k$) delivered natively to a single atom by an individual quantized field excitation (photon).

5.2 The Physics of Doppler Cooling

By utilizing detuned laser configurations where the driving laser frequency is tuned slightly below the atomic resonance frequency ($\omega_L < \omega_0$), we exploit the kinematic Doppler effect to cool localized matter. An atom moving directly toward a counter-propagating laser beam perceives the incoming light as blue-shifted into exact resonance. The atom absorbs the photon, receiving a discrete deceleration momentum kick of $-\hbar k$.

The subsequent spontaneous emission occurs randomly across the spherical harmonics (Y_{1m}) of the atomic dipole field. Over many operational cycles, this randomized spatial emission averages its net momentum transfer to zero, resulting in a continuous, isotropic reduction of the atom's center-of-mass velocity (optical molasses). This cooling mechanism hits two fundamental thermal floors:

The Doppler Limit: The thermal floor dictated strictly by the natural linewidth γ of the underlying electronic transition:

$$T_D = \frac{\hbar\gamma}{2k_B} \tag{82}$$

The Recoil Limit: The fundamental kinetic floor where the discrete quantum bounce of a single emitted photon prevents further standard laser cooling:

$$T_R = \frac{\hbar^2 k^2}{2mk_B} \tag{83}$$

To bypass the Doppler limit, counter-propagating laser configurations generate spatial polarization gradients (standing waves). As an atom moves through this gradient, multi-photon transitions force it to continuously climb potential energy hills, converting kinetic energy into potential energy before being optically pumped back to a lower state (Sisyphus cooling) [20, 21]. Lowering this thermal velocity shrinks the atom's spatial wave packet, providing the exact boundary conditions needed to lock it into a mechanical trap.

5.3 Extreme Tight Confinement: The Lamb-Dicke Regime

When an atom is cooled and deeply confined within a localized potential trap to a region significantly smaller than its own de Broglie wavelength, quantum mechanics completely overrides classical kinematic emission. We define this deeply confined state via the dimensionless Lamb-Dicke parameter: $\eta = k\Delta x \ll 1$ [22].

$$\eta = k\Delta x = \sqrt{\frac{\omega_{\text{recoil}}}{\omega_{\text{trap}}}} \ll 1 \tag{84}$$

We evaluate how this extreme tight confinement alters the radiation properties by performing an explicit Taylor expansion on the spatial plane-wave phase operator truncated to the lowest non-vanishing orders of the Lamb-Dicke approximation:

$$e^{i\eta(\hat{a}+\hat{a}^\dagger)} \approx \hat{I} + i\eta(\hat{a} + \hat{a}^\dagger) + O(\eta^2) \tag{85}$$

Because $\eta \ll 1$, the identity operator $\hat{I}$ completely dominates the field interaction matrix element. This forces the electronic emission to occur almost exclusively on the elastic carrier line ($|n\rangle \rightarrow |n\rangle$), completely suppressing motional sidebands ($|n\rangle \rightarrow |n \pm 1\rangle$), which would otherwise represent the exchange of vibrational quanta (phonons) with the trap.

This mechanism can be fully explained by integrating Heitler's gauge separation framework:

The Longitudinal Trap Field ($\mathbf{E}_L$): The trapped ion is rigidly secured by the static or radio-frequency electric potentials of the trap electrodes. This is a purely irrotational, longitudinal interaction that dictates the external mechanical, motional eigenstates ($|n\rangle$) of the atom.

The Transverse Radiation Field ($\mathbf{E}_T$): The probing laser or emitted radiation is an independent solenoidal, propagating transverse gauge wave that drives internal electronic orbital transitions.

In the strict Lamb-Dicke regime, the longitudinal trapping field ($\mathbf{E}_L$) is overwhelmingly stiff compared to the mechanical momentum kicks delivered by the transverse radiation field ($\mathbf{E}_T$). Because this external longitudinal binding structure is so rigid, the transverse radiation field can no longer shake or displace the atom's center of mass. The mechanical recoil momentum $\hbar k$ of the photon is instantly transferred to the entire macroscopic trap structure rather than the individual atom. Because the mass of the trap apparatus is effectively infinite, the kinetic recoil energy penalty vanishes entirely ($E_{\text{recoil}} \rightarrow 0$), eliminating Doppler broadening. The atom's internal radiation profile is completely insulated and decoupled from its external physical motion.

6 Weak Field limit of General Relativity

While our taxonomic framework has thus far interrogated electromagnetic vector fields interacting with deeply confined atomic spinors, the geometric language of wavefront topologies and source symmetries extends naturally to spatial perturbations within the spacetime metric itself. In moving from the vector gauge domain to the gravitational tensor domain, we begin with the standard Newtonian viewpoint where gravity is treated explicitly as a force. As we shall demonstrate, relaxing this framework does not merely introduce dynamic waves; rather, in the weak-field Newtonian limit, it reveals how the local structure of gravity is macroscopically perceived as a consequence of warped time.

In the Newtonian viewpoint we have gravity as a force. We can write:

$$m_I \frac{d^2x}{dt^2} = F = m_G g(x) \tag{86}$$

where g is the gravity field. m_I is the inertial mass and m_G is the gravitational mass. Galileo first established $m_I = m_G$. We write gravitational field as:

$$g(x) = -\sum_i G m_i \frac{x - x_i}{|x - x_i|^3} \tag{87}$$

at some test point. Gravitation potential $\phi(x)$ is related with field as

$$g = -\nabla\phi = -\left(\frac{\partial\phi}{\partial x}\hat{i} + \frac{\partial\phi}{\partial y}\hat{j} + \frac{\partial\phi}{\partial z}\hat{k}\right) \tag{88}$$

Law of gravitation; Integral form :

$$\phi(x) = -G \int \frac{\rho(x')d^3x'}{|x - x'|} \tag{89}$$

Differential form:

$$\nabla^2\phi = 4\pi G\rho(x) \quad \text{where} \quad \nabla^2 = \frac{\partial^2}{\partial x^2} + \frac{\partial^2}{\partial y^2} + \frac{\partial^2}{\partial z^2} \tag{90}$$

Gravity as spacetime curvature : freely falling bodies move along spacetime geodesics, i.e. curves of extremal proper time.

Curve $x^\mu(\lambda)$ where $\mu = 0, 1, 2, 3$ and

$$\tau = \int \left[\sum_\mu \sum_\nu g_{\mu\nu}(x) \frac{dx^\mu}{d\lambda} \frac{dx^\nu}{d\lambda} \right]^{1/2} d\lambda \tag{91}$$

We get from Euler-Lagrange equations the path of extremal proper time

$$\frac{d^2x^\mu}{d\tau^2} = -\frac{1}{2} g^{\mu\nu} \left(\frac{\partial g_{\beta\nu}}{\partial x^\alpha} + \frac{\partial g_{\alpha\nu}}{\partial x^\beta} - \frac{\partial g_{\alpha\beta}}{\partial x^\nu} \right) \frac{dx^\alpha}{d\tau} \frac{dx^\beta}{d\tau} \tag{92}$$

and

$$\begin{aligned} d\tau^2 = {} & g_{00}(dx^0)^2 + g_{11}(dx^1)^2 + g_{22}(dx^2)^2 + g_{33}(dx^3)^2 \\ & + 2g_{01}(dx^0)(dx^1) + 2g_{02}(dx^0)(dx^2) + 2g_{03}(dx^0)(dx^3) \\ & + 2g_{12}(dx^1)(dx^2) + 2g_{13}(dx^1)(dx^3) + 2g_{23}(dx^2)(dx^3) \end{aligned} \tag{93}$$

4×4 metric tensor is $g_{\mu\nu}$ where all the indices α, β, μ, ν run from 0 to 3. We can relate Newton's law to this form of GR where we have derivatives of metric tensor components. $\frac{d^2x}{dt^2} = g = -\nabla\phi$ or we could also write $\frac{d^2x'}{dt^2} = g^i$ where $i = 0, 1, 2, 3$

In curved space time geodesics may start out parallel but then diverge as on a saddle surface or converge as on a spherical surface. So up to now we were describing how curved spacetime tells matter how to move now we will explore how mass tells spacetime how to curve. Or in other words how does spacetime curve in response to matter i.e. what determines $g_{\mu\nu}(x)$. The answer comes from field equations.

$$G^{\mu\nu} = 8\pi G T^{\mu\nu} \tag{94}$$

Let's look at the content and nature of field equations. The theory shall pass all experimental tests. It should reduce to Newtonian gravity for weak fields and slow motion. Laws of physics should be the same in all inertial frames. So the theory should locally satisfy Special Relativity. Gravitational fields can induce or modify gravitational fields. That is field equations are non-linear. Field itself has the energy or gravity carries with itself its source energy. The theory must be consistent with energy-momentum conservation. Or energy-momentum cannot be created or destroyed without compensation.

$$T^{\mu\nu} = \begin{pmatrix} \rho & p_x & p_y & p_z \\ p_x & \sigma_{xx} & \sigma_{xy} & \sigma_{xz} \\ p_y & \sigma_{xy} & \sigma_{yy} & \sigma_{yz} \\ p_z & \sigma_{xz} & \sigma_{yz} & \sigma_{zz} \end{pmatrix} \tag{95}$$

Let's look more closely to $T^{\mu\nu}$. We define relativistic energy density U. But as energy is not a Lorentz invariant as it is part of energy-momentum 4-vector likewise energy density is not a Lorentz scalar. $U = \frac{\text{Energy}}{\text{Volume}}$ So as volume gets Lorentz contraction and if momentum is zero in some frame S, then in S' it is $U' = \gamma^2 U$ we get a square of the Lorentz factor in fact one gamma is coming from energy and the other is coming from the volume. These two parts of gamma tell us that stress-energy-momentum tensor has two indices.

In a Lorentz frame $T^{\mu\nu}$ will be a 4×4 matrix whose first row as well as first column is energy density and momentum density and the rest 3×3 matrix would be containing stress and pressure terms. By dimensional analysis Energy density $= \frac{\text{Energy}}{\text{Volume}} = \frac{\text{Force . distance}}{\text{Area . distance}} = \frac{\text{Force}}{Area} =$ Pressure or Stress

In GR energy-momentum-stress all participate in the energy conservation. This also tells us that source of gravity should also include pressure. Let's discuss a bit about negative pressure. If you take an elastic rubber band and pull it out then you have to do work on the system. Take a box of gas and you let it expand then the system does work on you. Similarly if we have negative pressure in some region it can create repulsive gravitational field. Universe might be filled with such substance of negative pressure which propels our universe to accelerated expansion.

$G^{\mu\nu} = 8\pi G T^{\mu\nu}$ The Einstein tensor up to a trivial redefinition a tensor that is linear in $\frac{\partial^2 g_{\mu\nu}}{\partial x^\alpha \partial x^\beta}$ and contains no higher derivatives of curvature. So in the Newtonian limit:

$$G^{00} \to \left(\frac{\partial^2 g_{00}}{\partial x^2} + \frac{\partial^2 g_{00}}{\partial y^2} + \frac{\partial^2 g_{00}}{\partial z^2} \right) \tag{96}$$

in weak field Newtonian limit. Hence

$$G^{00} = 8\pi G T^{00} = 8\pi G U = 8\pi G \rho \tag{97}$$

$$g_{00} = -\left(1 + \frac{2\phi}{c^2}\right) \tag{98}$$

$$2\nabla^2 \phi = 8\pi G \rho \tag{99}$$

$$\nabla^2 \phi = 4\pi G \rho \tag{100}$$

So, we obtain the Newtonian gravitation. The cost for a time dependent metric is that time is warped:

$$d\tau^2 = \left(1 + \frac{2\phi}{c^2}\right) dt^2 - \frac{1}{c^2}\left(dx^2 + dy^2 + dz^2\right) \tag{101}$$

So, for Newtonian gravity we get from time warping and whereas for the Black hole description we go for space curvature. Time tells the metric how to fall in a gravity field.

6.1 Accelerating Mass in General Relativity (GR)

Under linearized GR, we relax the static assumption $\partial_0 \to 0$ of the Newtonian limit to evaluate dynamic, time dependent fields. The fundamental geometric entity is the full metric tensor $g_{\mu\nu}$ which we decompose into a flat background Minkowski metric $\eta_{\mu\nu} = \text{diag}(-1, 1, 1, 1)$ and a small dynamic field perturbation $h_{\mu\nu}$.

$$g_{\mu\nu} = \eta_{\mu\nu} + h_{\mu\nu}, \quad |h_{\mu\nu}| \ll 1 \tag{102}$$

To uncouple the linearized field equations we invoke the trace-reversed metric perturbation defined as $h_{\mu\nu} \equiv h_{\mu\nu} - \frac{1}{2}\eta_{\mu\nu} h^\alpha_\alpha$, where h^α_α represents the trace.

Driven by a localized stress-energy-momentum tensor $T_{\mu\nu}$, the spacetime field is locally governed by the inhomogeneous wave equation:

$$\Box \bar{h}_{\mu\nu} = -\frac{16\pi G}{c^4} T^{\mu\nu} \tag{103}$$

This is analogous to vector gauge coupling $J^\mu A_\mu$ so the action for interaction becomes:

$$S_{\text{int}} = -\frac{1}{2c} \int T^{\mu\nu}(x) h_{\mu\nu}(x) d^4x \tag{104}$$

Because $h_{\mu\nu}$ is a symmetric 4×4 matrix, it initially possesses 10 independent components. By applying an infinitesimal coordinate transformation $x^\mu \to x^\mu + \xi^\mu$, we exploit the gauge freedom of linearized gravity to eliminate 4 unphysical degrees of freedom. We enforce this explicitly by imposing the Lorentz gauge condition $\partial_\mu \bar{h}^{\mu\nu} = 0$, which reduces the independent components to 6.

Just as we isolated the true propagating photon by dropping the longitudinal field E_L in electromagnetism in a similar vein we can isolate true propagating graviton in the vacuum $T_{\mu\nu} = 0$ by discarding the non-propagating longitudinal Newtonian and gravitomagnetic potentials. This is achieved by selecting the Transverse-Traceless (TT) gauge, which enforces 4 additional constraints: $h_{0\mu} = 0$ (Purely Spatial), $h^\mu_\mu = 0$ (Traceless). Because the metric is traceless in this gauge, the trace-reversal operation vanishes identically meaning $\bar{h}^{TT}_{\mu\nu} = h^{TT}_{\mu\nu}$.

These constraints eliminate 8 redundant components leaving exactly 2 physical independent transverse polarizations denoted as the plus h_+ and cross h_X strains of the spacetime metric[23].

$$h_{\mu\nu}^{TT} = \begin{bmatrix} 0 & 0 & 0 & 0 \\ 0 & h_+ & h_\times & 0 \\ 0 & h_\times & -h_+ & 0 \\ 0 & 0 & 0 & 0 \end{bmatrix} \tag{105}$$

This radical filtering of unphysical states forces a strict boundary on permissible radiation modes, because total mass-energy, linear momentum and angular momentum are globally conserved ($\partial_\nu T^{\mu\nu} = 0$), gravitational monopole ($l = 0$), and dipole ($l = 1$) radiations are completely forbidden. The lowest allowed radiating channel is the quadrupole mode ($l = 2$) which maps to spin-weighted harmonics (${}_{-2}Y_{lm}$) to accommodate the tensor polarizations of a massless, spin-2 graviton field.

For a macroscopic distribution of matter the radiation is driven by the continuous second time derivative of the mass quadrupole moment tensor:

$$Q_{ij} = \int \rho(x)(3x_{ij} - r^2\delta_{ij})d^3r \tag{106}$$

To demonstrate how these localized mass-energy distributions drive tensor radiation, we analyze a cosmic pulsar spinning with an angular frequency Ω around the z-axis. For a perfectly spherical mass distribution with a uniform density or isotropic boundary layers, the off-diagonal components of the mass quadrupole moment tensor vanish identically, while the diagonal components remain completely static ($Q_{xx} = Q_{yy} = Q_{zz} =$ constant). Because the Larmor-like emission profile under general relativity requires time-varying dynamics, the second time derivative drops to zero ($\ddot{Q}_{ij} = 0$), proving that a perfectly spherical spinning source cannot generate gravitational waves.

Conversely, we evaluate a non-axisymmetric oblate spheroidal pulsar characterized by a triaxial moment of inertia structure, where an equatorial asymmetry parameter $\epsilon = (I_{xx} - I_{yy})/I_{zz}$ dictates the geometric deformation. Tracking the time-dependent rotation across the xy-plane yields the non-zero oscillating quadrupole tensor components $Q_{xx} = -Q_{yy} = \frac{3}{2}\epsilon I_{zz}\cos(2\Omega t)$ and $Q_{xy} = Q_{yx} = \frac{3}{2}\epsilon I_{zz}\sin(2\Omega t)$ Differentiating these components twice reveals that the source drives spacetime strains at exactly twice the foundational mechanical rotation frequency (2Ω), where the prefactor amplitude shifts to track our trace-free normalization definition established in Eq. (105):

$$\ddot{Q}_{xx} = -6\epsilon I_{zz}\Omega^2\cos(2\Omega t) \quad \text{and} \quad \ddot{Q}_{xy} = -6\epsilon I_{zz}\Omega^2\sin(2\Omega t) \tag{107}$$

When these source dynamics are integrated into the asymptotic trace-reversed metric perturbations, they synthesize the deterministic, transverse-traceless coherent strains h_+ and $h_\times$ propagating through the manifold toward infinity, evaluated here specifically for an observer situated along the primary rotation axis (z-axis) to map the pure co-axial strain amplitudes:

$$h_+(t) = \frac{4G\Omega^2}{c^4 r}\epsilon I_{zz}\cos(2\Omega t_{\text{ret}}) \quad \text{and} \quad h_\times(t) = \frac{4G\Omega^2}{c^4 r}\epsilon I_{zz}\sin(2\Omega t_{\text{ret}}) \tag{108}$$

where $t_{\text{ret}} = t - r/c$ marks the causal retarded time boundary. This mechanical framework provides the explicit geometric receipt of cosmic spin-2 radiation channels.

For a quantum matter source undergoing a state transition $|\Psi_i\rangle \to |\Psi_f\rangle$, the classical source is replaced by the transition stress-energy tensor operator matrix element:

$$T_{fi}^{\mu\nu}(x) = \langle\Psi_f|\, T^{\mu\nu}(x)\,|\Psi_i\rangle \tag{109}$$

During the transition, the spatial superposition of the initial and final mass-energy wavefunctions creates a real time-dependent quadrupole oscillation of the localized matter-energy field. This transition tensor oscillates at the Bohr frequency ω_{fi}, driving the vacuum modes of the spin-2 tensor field to emit an on-shell, discrete quanta of spacetime radiation, a graviton. Because of the underlying tensor geometry calculating this emission profile requires spin weighted spherical harmonics (${}_{-2}Y_{lm}$) rather than standard scalar or vector harmonics, perfectly mapping the quadrupole radiation signatures to the spatial geometry of the source's mass-energy transitions.

Note this when we state that the field is static, it means that all time derivatives of the metric vanish ($\partial_0 \rightarrow 0$)or($\frac{\partial}{\partial x^0} \rightarrow 0$). Space itself is not expanding, contracting or rippling. Because space is completely static, the spatial components of the metric (g_{xx}, g_{yy}, g_{zz}) collapse back to their flat, unbent value (-1). Space is flat. However, the time component g_{00} is not flat, it holds the Newtonian potential $g_{00} = -(1 + 2\phi)$. When a test particle moves through this environment, its acceleration is dictated by how proper time ticks from one coordinate point to another. Because ϕ varies from place to place (stronger near a mass, weaker far away), clocks tick at different speeds depending on their spatial location.

Therefore, setting $\partial_0 \rightarrow 0$ leaves us with an environment where space bending is completely gone and only time warping remains. This time warp is what we macroscopically perceive as classical Newtonian gravity.

How does curved spacetime geometry modify the asymptotic decoupling threshold of multipole radiation? Curved spacetime stretches the radiation's clean escape into a long, blurry exit zone. In flat space, multipole waves snap free from their source instantly. Near a massive object, curved space acts like a thick, warped lens. This geometry traps high-energy waves and shifts their frequencies. Crucially, the waves also bounce off the curvature of space itself. This creates a trailing echo that delays their escape. Radiation never truly detaches cleanly from a curved background. Instead, it carries a physical imprint of the gravity it survived.

Note that when we evaluate a time-independent metric ($\partial_0 \rightarrow 0$), it does not imply that spatial geometry is perfectly flat, as static, massive configurations like the Schwarzschild metric still exhibit heavy spatial curvature. Rather, within the weak-field Newtonian limit, the leading-order acceleration of a slow test particle depends strictly on the spatial gradient of the time-warping metric component g_{00} [24]. Proper time ticks at different speeds depending on the spatial location. Therefore, setting $\partial_0 \rightarrow 0$ isolates a regime where the macroscopic path trajectories of slowly moving matter can be modeled entirely by this time warp, which we macroscopically perceive as classical Newtonian gravity.

7 The Radiation Zoo

When source geometries alter or statistical thermal equilibria are reached, the outward topology of the radiation field changes fundamentally, breaking away from standard spherical assumptions.

Cylindrical Wavefronts (Line Sources)

For line sources possessing translational invariance along the z-axis, scalar spherical harmonics Y_{lm} are replaced by Azimuthal Fourier modes ($e^{im\phi}$) and Cylindrical Bessel/Hankel functions (J_m, H_m). This geometry breaks the standard inverse-square law: the radiation intensity decays slowly as $1/R$. Furthermore, odd dimensions in the reduced Huygens principle manifest a 2D wave "wake/tail" effect, meaning a sharp pulse leaves a residual trailing field behind. Physical expressions include current-carrying wires and cosmic strings.

Planar Wavefronts (Sheet Sources)

Infinite sheet sources exhibit complete spatial uniformization across the xy-plane. The wave equation collapses into a simple 1D ordinary differential equation solved by plain exponentials ($e^{i(kz-\omega t)}$). Crucially, planar wavefronts experience zero spatial energy decay, maintaining a constant intensity profile ($I \propto 1$). This topology is realized in relativistic laser cavities and cosmic domain walls.

Atomic and Nuclear Transitions in Quantum Electrodynamics (QED)

Within this PZW-dressed representation, quantum transitions occur through discrete multipole channels, mapping cleanly across vastly different energy scales:

Electric Dipole ($E1$) Radiation ($l = 1$): Dictated by parity violation between states. The radiation footprint exhibits a $\sin^2\theta$ geometric angular dependence mapped to $|Y_{1\pm1}|^2$.

Electric/Magnetic Quadrupole ($E2/M2$) Radiation ($l = 2$): Maps directly onto the geometric shapes of Y_{2m}, where the $E2$ channel preserves spatial parity while the $M2$ channel changes it [9, 10].

High-Energy Gamma (γ) Radiation: When the source engine shifts from atomic electronic shell reorganizations to sub-femtometer nuclear nucleon transitions, the emission scales into the ultra-high-frequency regime. Because

gamma emissions remain purely electromagnetic, they preserve identical geometric coupling profiles, adhering strictly to nuclear parity selection rules mapped via these exact multipole expansions.

Laguerre-Gaussian (LG) Fields and Cylindrical Singularities: Laguerre-Gaussian modes form a comprehensive family of paraxial cylindrical solutions characterized by an explicit helical phase factor $e^{i\ell\phi}$, where ℓ represents the integer topological charge. Due to a phase singularity at the central propagation axis, the field intensity self-extinguishes to form a perfectly dark core, producing a characteristic doughnut profile. Crucially, each spatial mode excitation carries a discrete, quantized orbital angular momentum (OAM) equal to $\ell\hbar$ per photon.

Cyclotron OAM Synthesis: Charged particles gyrating continuously within uniform magnetic fields establish a rotating current distribution. This circular kinematic footprint breaks standard wavefront uniformity, naturally embedding an explicit $e^{i\ell\phi}$ phase modulation into the outward tensor components. Relativistic synchrotron scaling utilizing helical undulator arrays upgrades this configuration into an OAM engine capable of synthesizing high-frequency X-ray and gamma vortices possessing massive topological charges. **Classical Accelerating Charges: Synchrotron and Cherenkov Engines**

In contrast to quantized state-hopping, continuous classical acceleration profiles emit a continuous spectrum. Because these macroscopic currents are governed by smooth charge distributions rather than discrete transitions, quantum Clebsch-Gordan coupling coefficients are entirely absent from classical electrodynamic calculations. This regime manifests distinct structural variations based on the velocity and medium of the accelerating charge:

Synchrotron Radiation: When ultra-relativistic charges ($\mathbf{v} \approx c$) undergo intense centripetal acceleration perpendicular to an external magnetic field ($\mathbf{a} \perp \mathbf{v}$), the standard Larmor dipole emission pattern undergoes extreme relativistic forward-beaming. The angular power distribution collapses into a highly collimated, razor-thin forward cone of angle $\theta \approx 1/\gamma$. Macroscopically, this flattens the local wavefront profile along the instantaneous orbital arc, producing intense, planar-like pulse segments.

Cherenkov Radiation: When a charged particle traverses a dielectric medium with a uniform velocity exceeding the phase velocity of light in that medium ($v > c/n$), it breaks local isotropic phase symmetry. The particle outruns its own local polarization fields, synthesizing a coherent, asymmetric, **conical shockwave wavefront**. The radiation geometry is locked strictly to a Mach-like cone angle dictated by $\cos\theta_C = 1/\beta n$, representing a purely hydrodynamic wavefront synthesis within a dielectric field.

Thermodynamic Fields: Thermal Cavity and Blackbody Radiation

When radiation fields reach complete thermodynamic equilibrium with surrounding matter within a closed cavity, individual wavefront histories are completely erased. The field collapses into a completely isotropic, randomized "field gas" governed by statistical mechanics rather than deterministic source geometry. The spectral energy distribution is mapped strictly by Planck's law:

$$u(\omega, T) = \frac{\hbar\omega^3}{\pi^2 c^3} \frac{1}{e^{\hbar\omega/k_B T} - 1} \tag{110}$$

Here, the spatial footprint exhibits absolute geometric uniformity across all angular degrees of freedom, transforming the localized radiation profile into a uniform statistical fluid density.

Macroscopic Cooperative and Cosmological Synthesis

While a solitary atom always emits spherically, cooperative collections of macroscopically ordered atoms (such as arrays in lasers, discharge tubes, and lenses) can synthesize perfect cylindrical or planar radiation fields via constructive phase interference. On a cosmological scale, these geometric transformations dictate extreme systemic topologies:

The Cosmic Microwave Background Radiation (CMBR): The ultimate thermodynamic relic field of the universe. It exhibits near-perfect isotropic blackbody symmetry across the cosmic horizon ($T \approx 2.73\,\mathrm{K}$), serving as an omnipresent, uniformly redshifted statistical field gas filling all spacetime.

Pulsar Gamma-Ray Bursts: Driven by intense, rotating magnetic field geometries of magnetars and neutron stars. Relativistic plasma streams accelerated along the star's magnetic poles force ultra-high-frequency gamma radiation into highly collimated, narrow jet topologies that sweep across space like cosmic beacons.

Horizon-Induced Thermodynamic Radiation: Unruh and Hawking Mechanisms When quantum fields are evaluated across non-inertial reference frames or curved spacetimes, radiation emerges not from a structural, accelerating material source, but from the global restructuring of the vacuum state. These phenomena bridge quantum field theory and thermodynamics through the geometry of causal horizons.

The Unruh Effect (Rindler Horizon Transformation): An observer undergoing uniform proper acceleration a through a Minkowski vacuum perceives an isotropic thermal bath of particle coordinates. This transformation is mathematically executed by mapping inertial Minkowski modes to non-inertial Rindler wedge coordinates using Bogoliubov coefficients. The acceleration establishes a sharp causal Rindler horizon, shifting the field density matrix from a pure vacuum state into a mixed thermal state governed by the Fulling-Davies-Unruh temperature:

$$T_U = \frac{\hbar a}{2\pi k_B c} \tag{111}$$

The spatial topology of this field behaves as a completely randomized, isotropic statistical gas restricted entirely within the observer's active causal wedge.

Hawking Radiation (Event Horizon Redshift): By the strong Equivalence Principle, a stationary observer outside a Schwarzschild black hole horizon experiences a constant proper acceleration to resist gravitational collapse, mapping the vacuum breakdown directly to a curved geometry. Rather than virtual particle-pair splitting at the boundary, this radiation arises from the exponential gravitational redshift of wave modes climbing out of the steeply curved spacetime manifold toward infinity. The resulting field matches a perfect blackbody spectrum at the Hawking temperature:

$$T_H = \frac{\hbar \kappa}{2\pi k_B c} = \frac{\hbar c^3}{8\pi G M k_B} \tag{112}$$

where $\kappa = \frac{c^4}{4GM}$ is the surface gravity of the event horizon. This mechanism establishes that horizons erase geometric memory, converting localized mass-energy into pure, undecoupled thermodynamic field gas emissions that drive black hole evaporation.

Does radiation possess a memory? At first glance, a photon escaping into the void appears to be a fleeting entity, a transient packet of energy completely uncoupled from its past. Yet, when we interrogate the gauge and tensor fields fleeing toward infinity, we discover that radiation is the ultimate cosmic archivist. Indeed, decoupled photons bear the permanent physical burden of the engines that birthed them, encoding structural secrets within their very quantum coordinates. By reverse-engineering their properties, we can dismantle the inverse scattering problem: a photon's energy and frequency act as a physical receipt of specific atomic transitions or nuclear decay channels, while its polarization maps out the exact vector distribution of the source's local magnetic fields. Even the arrival phase of the wave envelope retains an unbroken log of the source's macroscopic kinematics, allowing us to reconstruct the precise structural motion of highly relativistic engines like rapidly rotating pulsars.

Yet, what happens when radiation falls into complete thermodynamic equilibrium, collapsing into a randomized statistical fluid? In this regime, standard thermalization acts as a brutal cosmic eraser; individual wavefront histories are wiped clean, and the explicit atomic signatures of the parent matter are lost forever to the dictates of Planck's law. However, the universe refuses to forget entirely. Consider the Cosmic Microwave Background Radiation (CMBR). While these ancient thermal photons lost the micro-memory of the specific electrons that shook them free, they sealed a macro-memory of the cosmos itself. Across billions of light-years, the CMBR preserves the system-wide snapshot of the infant universe through faint temperature anisotropies and structural acoustic oscillations—fossilized plasma sound waves that map the primordial distribution of matter.

The ultimate expression of this macro-memory is etched into the geometric polarization modes of this ancient light. Standard density fluctuations generate symmetric, curl-free E-mode (gradient) polarization patterns across the sky. However, the true holy grail for the next generation of physicists lies in the elusive B-mode (curl) polarization. These subtle, twisting, whirlpool-like imprints cannot be generated by standard matter density alone; primordial B-modes require the violent stretching of spacetime caused by primordial gravitational waves during Cosmic Inflation. Alternatively, as this light traverses the cosmos, the gravity of intervening dark matter structures bends its path, lensing E-modes into secondary B-modes and providing a structural map of the cosmic web. By separating these pure gradient E-modes from curling B-modes, researchers are not just catching escaping photons—they are reading a permanent, topological archive of the universe's first fraction of a second and its grandest structures,

proving that radiation's global geometry retains the indelible imprints of the history it survived. The complete overarching taxonomy of these diverse radiation fields, along with their matching geometric symmetries, decay laws, and cosmic engines, is synthesized for comparison in Table 2.

Table 2: Structural Synthesis of Radiation Frameworks

Topology / Engine	**Geometric Symmetry**	**Decay Law**	**Physical / Cosmic Engine**
Spherical	$Y_{lm}/{}_{-2}Y_{lm}$	Intensity $\propto 1/R^2$	Atoms, Nuclear γ-Decay, Black Holes
Cylindrical	Azimuthal $e^{im\phi}$	Intensity $\propto 1/R$	AC Wires, Cosmic Strings, 2D Wave Tails
Planar	Exponential e^{ikz}	Intensity $\propto 1$	Lasers, Domain Walls, Synchrotron Arcs
Conical Shockwave	Mach Cone $\cos\theta_C = \frac{1}{\beta n}$	Medium Constrained	Cherenkov Particle Medium Shockwaves
Collimated Jet	Axial Coherent Focus	Highly Directional	Polar Accelerator Plasmas, Pulsar γ Beacons
Isotropic Field Gas	Uniform Statistical Space	Uniform Density $u(\omega)$	Cavity Thermal Blackbodies, Cosmic CMBR
Lamb-Dicke	Carrier-Locked $\hat{I}$	Recoil-Free	Trapped Ions, Mössbauer Confinement
Horizon-Induced	Isotropic Thermal Space	Mass-Dependent Decay	Evaporating Black Holes, Rindler Fields

8 Outlook

The exploration of radiative boundary regimes expands far beyond linear perturbations, unlocking extreme domains where fields fundamentally rewrite the quantum vacuum. At the absolute limit of field intensity, the vacuum undergoes macroscopically observable phase transitions; under the critical electric thresholds of the non-perturbative Schwinger effect, fields break down entirely to spontaneously materialize electron-positron pairs directly out of empty space. This non-classical synthesis of matter from pure gauge fields marks an elite boundary where radiation ceases to be a passive vehicle for energy and instead becomes an active structural engine of the universe.

Furthermore, exploring the microscopic topology of radiation introduces rich geometric frameworks such as skyrmionic and non-trivial knotted electromagnetic fields, where the field lines themselves form stable, self-localized topological structures. Mapping these complex geometries onto intense cosmic accelerators, vacuum birefringence channels, and structured laser fields reveals that radiation is an immensely vast, highly dynamic field gas capable of morphing into complex spatial phases. Bridging these high-field non-linear frameworks with the engineering constraints of confined quantum systems will inevitably drive the next generation of deep-space communications, vacuum polarization engines, and quantum state manipulation architectures.

Acknowledgements

The author expresses sincere gratitude to Professor Dmitry Budker for highly intuitive and inspiring discussions during the Bad Honnef conference on Dark Intersections, which significantly enriched the conceptual clarity of this work. A separate note of thanks is extended to the Physics Academy of the North East for graciously providing the opportunity to present, share, and refine these ideas within the community.

AI Disclosure Statement

In preparing this work, the author used Gemini for structural proofreading. The author subsequently reviewed and revised the content as necessary and accepts full responsibility for the final published work.

References

[1] J. J. Sakurai and Jim Napolitano, Modern Quantum Mechanics, 3rd ed. (Cambridge University Press, Cambridge, United Kingdom, 2020).

[2] Catalina Curceanu, James D. Gillaspy, and Robert C. Hilborn, "Resource Letter SS-1: The spin-statistics Connection", American Journal of Physics 80, 561–577 (2012).

[3] Roy J. Glauber, "Coherent and incoherent states of the radiation field", Physical Review 131, 2766–2788 (1963).

[4] CMS Collaboration, "A portrait of the Higgs boson by the CMS experiment ten years after the discovery", Nature 607, 60–68 (2022).

[5] Peter W. Higgs, "Spontaneous symmetry breakdown without massless bosons", Physical Review 145, 1156–1163 (1966).

[6] Abdelhak Djouadi, "The anatomy of electro-weak symmetry breaking. I: The Higgs boson in the Standard Model", Physics Reports 457, 1–216 (2008).

[7] Walter Heitler, The Quantum Theory of Radiation, 3rd ed. (Oxford University Press, Oxford, 1954).

[8] NIST, Atomic spectroscopy, sec. 2, frequency, wavenumber, wavelength, eq. (1), in atomic spectroscopy—introduction, https://nist.gov, 2026.

[9] NIST, Atomic spectroscopy, sec. 17, spectral lines: Selection rules, intensities, transition probabilities, values, and line strengths, https://nist.gov, 2026.

[10] Kenneth S. Krane, Introductory Nuclear Physics, (John Wiley & Sons, New York, 1988).

[11] Masud Mansuripur and Per K. Jakobsen, "Electromagnetic radiation and the self-field of a spherical dipole oscillator", American Journal of Physics 88, 693–701 (2020).

[12] R. de Melo e Souza, M. V. Cougo-Pinto, C. Farina, and M. Moriconi, "Multipole radiation fields from the Jefimenko equation for the magnetic field and the Panofsky–Phillips equation for the electric field", American Journal of Physics 77, 67–72 (2009).

[13] Edwin A. Power and Sigmund M. Zienau, "Coulomb gauge in non-relativistic quantum electrodynamics and the shape of spectral lines", Philosophical Transactions of the Royal Society of London. Series A, Mathematical and Physical Sciences 251, 427–454 (1959).

[14] M. Kachelrieß and M. N. Malmquist, "Using covariant polarisation sums in QCD", The European Physical Journal Plus 137, 89 (2022).

[15] J. D. Jackson, "From Lorenz to Coulomb and other explicit gauge transformations", American Journal of Physics 70, 917–928 (2002).

[16] A. Vukics, G. Kónya, and P. Domokos, "The gauge-invariant Lagrangian, the Power–Zienau–Woolley picture, and the choices of field momenta in nonrelativistic quantum electrodynamics", Scientific Reports 11, 16337 (2021).

[17] Robert H. Dicke, "Coherence in spontaneous radiation processes", Physical Review 93, 99–110 (1954).

[18] Yu-Kun Lu, Hanzhen Lin, and Wolfgang Ketterle, "Fundamental impossibility of a superradiant neutrino Laser", Physical Review Letters 137, 101804 (2026).

[19] J. Aasi et al., "Gravitational waves from known pulsars: Results from the initial detector era", The Astrophysical Journal 785, 119 (2014).

[20] Paul D. Lett, Richard N. Watts, Christoph I. Westbrook, William D. Phillips, Phillip L. Gould, and Harold J. Metcalf, "Observation of atoms laser cooled below the doppler limit", Physical Review Letters 61, 169–172 (1988).

[21] Jean Dalibard and Claude Cohen-Tannoudji, “Laser cooling below the doppler limit by polarization gradients: simple theoretical models”, Journal of the Optical Society of America B 6, 2023–2045 (1989).

[22] Dietrich Leibfried, Rainer Blatt, Christopher Monroe, and David J. Wineland. Quantum dynamics of single trapped ions. Reviews of Modern Physics, 75(1):281–324 (2003).

[23] Benjamin P. Abbott et al., “Observation of gravitational waves from a binary black hole merger”, Physical Review Letters 116, 061102 (2016).

[24] Sean M. Carroll, Lecture notes on general relativity (1997).